PONTIFICIA UNIVERSIDAD CATÓLICA DEL PERÚ

Escuela de Posgrado

Assessment of Fresh and Hardened State Properties in Medium-Scale 3D Printing of Earth-Cement Mixtures with and without Jute Fibers

Tesis para obtener el grado académico de Maestra en Ingeniería y Ciencia de los Materiales que presenta:

María Valeria Burgos Pérez

Asesor:

Suyeon Kim De Aguilar

Lima, 2025

Informe de Similitud

Yo, Suyeon Kim De Aguilar, docente de la Escuela de Posgrado de la Pontificia Universidad Católica del Perú, asesor de la tesis titulada **"Assessment of Fresh and Hardened State Properties in Medium-Scale 3D Printing of Earth-Cement Mixtures with and without Jute Fibers"**, de la autora María Valeria Burgos Pérez, código PUCP: 20140533, alumna de la Maestría en Ingeniería y Ciencia de los Materiales, dejo constancia de lo siguiente:

- El mencionado documento tiene un índice de puntuación de similitud de 19%. Así lo consigna el reporte de similitud emitido por el software *Turnitin* el 12/03/2025.
- He revisado con detalle dicho reporte y la Tesis o Trabajo de Suficiencia Profesional, y no se advierte indicios de plagio.
- Las citas a otros autores y sus respectivas referencias cumplen con las pautas académicas.

Lima, 12 de marzo de 2025.

Kim De Aguilar, Suyeon	
DNI: 48816908	Firma
ORCID: 0000-0003-1621-1489	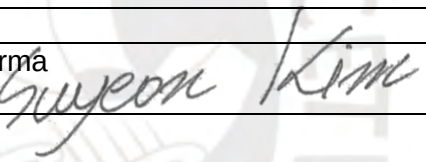

Resumen

Perú es un país sísmicamente activo que se caracteriza por una prevalencia desproporcionadamente alta de viviendas informales, gran parte de las cuales se construyen sin una supervisión adecuada durante el proceso de construcción. En este contexto, la manufactura aditiva (impresión 3D) surge como una metodología de construcción transformadora, que ofrece un proceso de construcción sustancialmente acelerado en relación con las técnicas convencionales y reduce significativamente el desperdicio de material. Sin embargo, su adopción generalizada se ve obstaculizada por desafíos críticos, en particular la alta demanda de cemento, aditivos y otros materiales esenciales, que aumentan los costos generales del proyecto. En respuesta a estas limitaciones, este estudio tiene como objetivo mejorar la eficiencia de los materiales minimizando el consumo de recursos y garantizando un rendimiento mecánico y reológico óptimo. La composición seleccionada comprende suelo arcilloso, agua y cemento, complementado por una investigación sobre los beneficios potenciales del refuerzo con fibra de yute. El marco de investigación implica una evaluación rigurosa de diferentes propiedades. En el estado fresco, las evaluaciones clave incluyen la prueba de impresión de filamentos, la prueba de veleta, la resistencia a la penetración y la caracterización reológica. Las métricas críticas de rendimiento, como el comportamiento de contracción, la resistencia a la compresión y las mediciones del ángulo de contacto, se examinarán al endurecer. Además, la resistencia a la erosión se evaluará sistemáticamente a través de pruebas de durabilidad, incorporando la prueba de inmersión, la prueba de capacidad de absorción y la prueba de erosión acelerada. Para corroborar estos hallazgos, se fabricarán especímenes impresos en 3D a mediana escala (~1 m^3 de volumen), con y sin fibras de yute, para determinar su influencia en el comportamiento de contracción y el rendimiento a largo plazo. Los resultados preliminares indican que el refuerzo de fibra mitiga significativamente el agrietamiento inducido por la contracción, mientras que el contenido de cemento ejerce una influencia decisiva en la integridad mecánica de los elementos de mediana escala. Estos conocimientos contribuyen a la evolución de materiales

sostenibles adaptados a los compuestos de suelo-cemento impresos en 3D, lo que mejora tanto la resiliencia estructural como la viabilidad medioambiental. Además, esta investigación establece una base crítica para futuras investigaciones, facilitando el desarrollo de mezclas sostenibles optimizadas que mejoren la eficiencia del refuerzo y mejoren la resistencia a la erosión, impulsando así la innovación en el campo de las tecnologías de manufactura aditiva.

Acknowledgments

Support for my thesis was provided by the project "WasiTek - Desarrollo de un sistema de construcción robótico autónomo para reconstrucción de viviendas post-desastre utilizando materiales locales mejorados con polímeros naturales extraídos de residuos industriales" (CONCYTEC Contract No. 178-2020-FONDECYT).

Agradecimientos

A Dios, por siempre demostrarme su presencia y amor. A mi mami, Elsa, porque sin ella no sería lo que soy, ni habría logrado lo que he logrado, eres un pilar fundamental en mi vida. A mis compañeros y amigos de Engineering & Heritage por las lecciones de vida, su gran apoyo y motivación. Al Sr. Miguel, por todo su apoyo y paciencia. A mi asesora, la profesora Suyeon Kim, por tener siempre fe en mí y ser mi mentora en el proceso de la tesis. Al profesor Rafael Aguilar, por darme la oportunidad de introducir en la investigación y sin el cual no estaría aquí. To my beloved parents-in-law, Kathy and Tony, for your support in the last step of this journey. And finally, to my sweet husband, Bradley, for being a supporter of my job and my best friend.

Table of Contents

Table of Figures

List of Tables

Chapter I

Introduction

1.1. Background

The billion has already been surpassed meaning one-quarter of the world's urban people live in unauthorized and unsupervised-by-professionals settlements, which means about 1.1 billion city residents inhabit areas developed without government oversight (Reckford & Aki-Sawyerr, 2023). The construction industry and governmental bodies must undertake substantial economic and technical initiatives to resolve this issue. However, current construction faces low productivity, low worker safety, lack of skilled human labor, high environmental impact, and massive energy and material consumption (McKinsey Global Institute, 2017). Autonomous construction processes would help address the housing shortage in a highly productive and safe manner. One of the most promising processes is additive manufacturing, commonly addresed as 3D printing, utilizing materials such as hydraulic concrete, geopolymer, or soil.

3D printing of concrete structures increases precision, improves safety, speeds up construction, and reduces costs by eliminating formwork and labor expenses. It also uses less material since printed elements don't need a solid interior (Alqenaee & Memari, 2022). Additionally, earth building has currently gained interest in the construction industry due to its low environmental impact and recyclability (McKinsey Global Institute, 2017).

Life cycle calculation reveals that earth-based building uses just 18-38% of the energy required for standard concrete and timber structures and cuts global climate impact by 75-82% (Faleschini et al., 2023). In 3D printing or additive manufacturing, dry items are mixed with water and pumped through a hose to create filaments. This filament is then extruded and guided to the desired location by a robotic arm or gantry frame system (Ji et al., 2023). Nevertheless, the advancement of earth construction is constrained by cost factors, challenges in obtaining insurance, and inadequate durability due to high water sensitivity. Designing a mixture that ensures both rapid casting and adequate strength in its dry state presents a significant challenge (Yemesegen & Memari, 2023).

Research has explored using biopolymers like alginate (Yemesegen & Memari, 2023) or a mix of hydraulic binders and additives to simulate cement curing. Therefore, cement could be an option. Portland cement-based matrices and geopolymer mortars and concretes are the most researched materials for additive construction (Yemesegen & Memari, 2023). The advancements in the seismic-resistance features have progressed as well. Companies like CyBe have already developed earthquake-resistant concrete material (CyBe Construction, 2024). Likewise, in 2023, COBOD printed a seismic-resistant house that could withstand a 9-magnitude earthquake in just 26 hours in Guatemala (Williams, 2023; Duboust, 2023).

To ensure the earth matrices for 3D printing are extrudable, a significant amount of water is required. Based on previous work with adobes, adding reinforcement to the matrix fiber was necessary for minimizing cracking caused by shrinkage during drying. To meet this requirement and reduce environmental impact, sisal, a readily available plant fiber with good mechanical properties, was chosen (Tu et al., 2023). However, adding flax fibers to self-compacting concrete has shown reduced workability and its impact on self-compaction characteristics in a fiber content-dependent manner. Furthermore, a notable improvement in mechanical properties and a slight reduction in unit weight were recorded (Tu et al., 2023).

1.2. Motivation

3D printing using earth as a building material has gained attention recently due to its potential for sustainable construction and waste reduction. Several case studies have demonstrated the viability of this technique. For example, in 2014, the Italian company WASP built the first 3D-printed house using raw earth. The process involved depositing layers of earth mixed with organic materials, creating sturdy and environmentally friendly structures.

3D printing with concrete has been widely researched and utilized in the construction industry. This technique enables the fabrication of complex structural elements and reduces construction times and costs. A notable example is the "The Office of the Future" project in Dubai, where a two-story office was 3D printed using a unique concrete mixture. This pioneering construction demonstrated the capability of 3D printing to create functional and aesthetically appealing buildings.

The implementation of 3D printing in construction is challenging. One of the critical challenges is the development of printing systems capable of working with granular materials like earth efficiently and accurately. Additionally, ongoing research is required to optimize the concrete mixes used in 3D printing, ensuring the strength and durability of the printed structures. Fortunately, significant progress has been made in improving the precision of printing systems, automating the process, and optimizing materials, leading to increased feasibility and acceptance of the technology in the construction industry.

3D printing in construction with earth and concrete presents enormous potential. In addition to housing construction, its use has been explored in constructing bridges, retaining walls, and complex structures. Creating custom designs and reducing waste and costs are significant advantages. Moreover, additive manufacturing permits the integration of unique architectural features and the ability to adapt to local and project-specific needs.

1.3. Objectives

1.3.1. General Objective

Optimization of mixing conditions of Soil-cement mixtures to apply to 3D printing construction and their mechanical and erosion resistance evaluations.

1.3.2. Specific Objectives

- Optimize the mixed design of a printable and stabilized soil-cement mortar paste.
- Assess how water and cement content affect 3D-printed soil-cement mixtures by analyzing the fresh and hardened state properties.
- Evaluate the effects of jute fiber addition and storage condition on cracking in soil-cement mixture on 3D printing
- Validate a medium-scale 3D printing with and without jute fibers.
- Evaluate the erosion resistance of the printed samples.

1.4. Organization

- Chapter 1 is the introduction, briefly describing this thesis's general objective, specific objectives, and organization.
- Chapter 2 presents the literature review and a summary of the theoretical framework. It introduces construction with 3D printing, concrete mixes, and other materials, regulations related to 3D printing, and 3D-printed constructions worldwide.
- Chapter 3 describes the materials, and the experimental plan including the mixed design and material preparation, the humidity control for weathering, and the test protocols.
- Chapter 4 explains the evaluation of properties in the fresh and hardened state divided into five stages comprising the first one the definition of printing parameters for non-reinforced soil-cement matrices including the printing speed test and the stacking test. The second stage is comprised of the fresh and hardened state characterization of non-reinforced and reinforced soil-cement matrices. Regarding the fresh-state

characterization, it included the shear stress, the over-time shear stress, the Vicat penetration test, and the rheology test. Likewise, the hardened-state includes the static elastic modulus, the compression test, and contact-angle characterization. To evaluate durability, is comprised of the immersion test, the absorption test, and the accelerated erosion test. In the third stage, is presented a medium-scale earthen 3D printing. In the fourth stage, a shrinkage cracking analysis is presented under different weathering conditions. Stage 5 presents a reinforced medium-scale earthen 3D printing.

- Chapter 5 presents the conclusions and recommendations regarding this thesis work.

Chapter II

Literature review

2.1. 3D Printing in Construction

3D printing in construction is a rapidly growing technology that allows for the creation of three-dimensional objects through a layering method. This process, referred to as additive manufacturing, uses computer-aided design (CAD) to construct objects layer by layer (Ross, 2024). The construction industry is benefiting from 3D printing advancements. 3D printing in construction provides various benefits, such as enhanced design forms, quicker construction timelines, and lower material costs (JK Cement, 2024).

Technology prints complete homes, modular structures, walls, offices, and bridges, increases construction industry spending, and advances in 3D printing technology, urban furniture. According to Global Market Insights (2024), the global 3D printing construction market is predicted to encounter substantial growth in the forthcoming years, determined by rapid urbanization. The following companies are key players in the 3D printing construction market: Yingchuang Building Technique (Shanghai) Co., Ltd. (Winsun), WASP, CyBe Construction, Sika AG, MX3D, Apis Cor, Contour Crafting Corp., Technology, Inc., XtreeE, COBOD International, Constructions-3D and ICON.

2.1.1. Overview of 3D printing in construction

This segment will cover some notable projects characterized by technological advancements, substantial budgets, and large scale, in addition to highlighting the companies with the most significant global presence. To begin with a review of each continent, America has the biggest number of important companies in the field, especially in the United States, such as ICON, Apis Cor, Mighty Building, Alquist, Pikus3D, S-Squared, Diamond Age, Contour Crafting, Changer-Maker, Building Machines, among others (Iribar, 2023; Morrison, 2024).

From there, will be point out, even more, the first two companies because the projects involved have a wide variety of purposes, from houses that have a sustainable design and architecture like House Zero (ICON, 2021) to houses that simulate Mars's surface like Mars Dune Alpha, ICON is trying to make their 3D printed houses suitable for any circumstance and customer (ICON, 2022). On the other side, Apis Cor, is looking for more accessible and affordable houses, selling more 3D printers than houses and had already built a two-story house standing at 32 feet tall. Apis Cor's printers are known for their versatility and ability to work in challenging environments (Apis Cor, 2024).

Regarding Europe, it can be included several companies such as CyBe, XtreeE, WASP, and COBOD (Ashcroft, 2024). The advent of 3D printing technology has renewed the construction area, facilitating the fabrication of intricate structures with unparalleled efficiency and cost-effectiveness. In 2022, XtreeE constructed five minimalist homes in Reims, France, each equipped with a kitchen, bed, and washrooms. They claimed these homes used 50% less concrete than traditional construction methods (Rincher, 2023). Other remarkable case was the eco-habitat printed by a Crane printer WASP in Massa Lombarda, Italy. This 3D printed construction project, by Rincher (2023), used natural, reusable, and recyclable materials, and is adaptable to any climate.

Asia has notable examples, like the world's first 3D-printed apartment building, created with WinSun's mix of cement, sand, fiber, and a proprietary additive. Construction

took place in Jiangsu Province, China, in 2015 and took 6 days at $161,000 (Rincher, 2023). WinSun claimed that at the time of building this project, it was the world's tallest 3D printed construction (Rincher, 2023). Another great example occurred in Bengaluru, India where the project utilized the COBOD BOD2 construction 3D printer. Constructed for approximately $27,500, the building's cost is about 40% less than it would have been using traditional construction methods (Rincher, 2023). It is noteworthy that a social media user residing nearby commented that the noise level during construction was "the bare minimum" (Rincher, 2023).

Africa was not excluded from the 3D printing industry, and great examples are the projects in Kilifi, Kenya, and Fianarantsoa, Madagascar (Rincher, 2023). The first one was printed with the Danish 3D printing company, COBOD. Alleged to be the world's largest 3D-printed reasonably priced housing complex (Peels, 2021), Mvule Gardens aims to reduce high rents for Kenya's urban population, 90% of whom rent their homes (Rincher, 2023; Kremenetsky, 2022). In the second project, in charge of the company Thinking Huts allied with COBOD, they developed Madagascar's first 3D printed school (Rincher, 2023).

Likewise, Oceania has not been indifferent to the industry, and Contour3D printed in May 2023 the first 3D-printed one-bedroom home with a Full Occupation certificate in Sydney, Australia (Contour3D, 2023). This project required 14 hours of print time over 2 days to complete the construction of the house. It was constructed using 24 tons of Contourcrete™, a proprietary 3D printable concrete developed by Contour3D. The home features exceptional comfort, incorporating a VersiClad roof and walls with PU insulation foam, which ensures a serene acoustic environment (Contour3D, 2023).

3D printing, initially linked with prototyping and bespoke consumer products, has seen a significant rise in its use within the construction sector (Hassan et al., 2024). Additive Construction (AC) is now utilized in a variety of projects, ranging from small-scale structures to medium-scale endeavors like 2000-square-foot houses (SQ4D LLC, 2024), bridges such as the one in China (Walsh, 2019), and entire communities (ICON, 2022). This technology's ability to convert virtual projects into real structures with high precision, decreased waste, speed, and improved site safety has spurred modernization in architectural and engineering fields, garnering substantial interest (Paritala et al., 2023). The United States currently leads in adopting Construction 3D Printing (C3DP), followed by the Netherlands (Wohlers

Associates, 2022). As illustrated in Figure 2.1, this technology is also being adopted in numerous other countries, with industry forecasts predicting an annual growth rate of 13.2% for C3DP from 2022 to 2027 (IndustryARC, 2022).

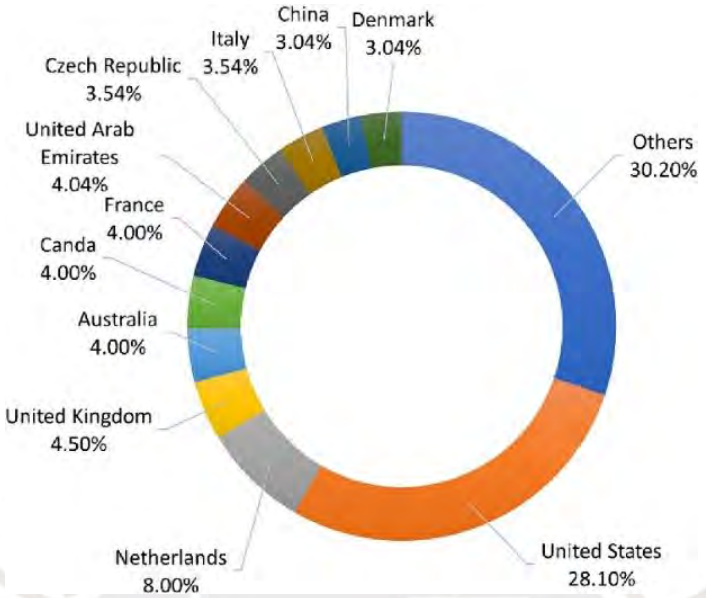

Figure 2.1. Global distribution of Construction 3D Printing by country (Wohlers Associates, 2022).

2.1.2. Regulatory Landscape in 3D Construction Printing

In this field, several standards published by the ISO can be considered in collaboration with ASTM International. The International Organization for Standardization (ISO) is a global association comprising national standards bodies (ISO/ASTM International, 2018). ISO is an independent, non-governmental entity that facilitates the collaboration of global experts to establish optimal practices. Their scope encompasses various domains including climate change, healthcare, quality management, and artificial intelligence. ISO's mission is to improve the quality of life by facilitating, ensuring safety, and making improvements (ISO, 2024). The line of chronological guidelines in additive manufacturing is shown in Figure 2.2.

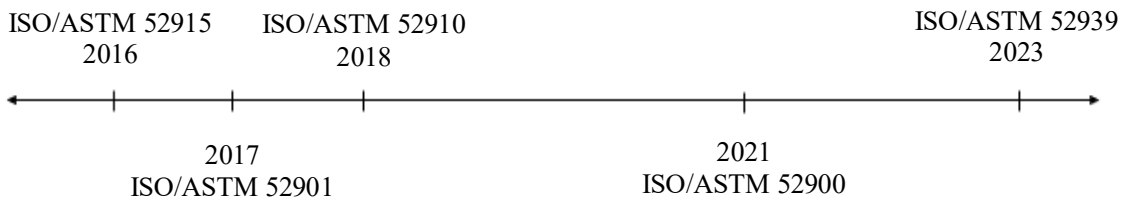

Figure 2.2. Timeline of 3D construction printing standards.

The ISO/ASTM 52915 (ASTM International, 2016) offered guidelines for employing additive manufacturing in the construction of buildings and infrastructure. It addressed essential topics such as material properties, process control, and quality assurance measures. However, ISO removed this guideline to emphasize the new ones' requirements. On the other hand, the ISO/ASTM 52901 (ASTM International, 2017) specifies requirements for the qualification of machine operators, materials, and processes in additive manufacturing. This standard is critical for ensuring that both personnel and materials meet the necessary qualifications and standards in construction applications.

Additionally, the ISO/ASTM 52910 (ASTM International, 2018) provided specific guidelines for design considerations in additive manufacturing. Key aspects covered the design process, material selection, and the requirements of additive manufacturing technologies. Meanwhile, the ISO/ASTM 52900 (ASTM International, 2021) serves as a foundational document, offering a thorough overview of additive manufacturing procedures, terminology, and definitions. This standard is essential for understanding the various facets of additive manufacturing, including its application in construction.

Lastly, the ISO/ASTM 52939 (ASTM International, 2023), labeled "Additive manufacturing for construction — Qualification principles — Structural and infrastructure elements", seeks to guarantee quality, safety, and competence in the 3D printing construction business. Specifically, it outlines quality assurance requirements for additive construction projects, focusing on structural and infrastructure elements produced using additive manufacturing techniques. Together, these standards establish a robust framework to ensure that 3D printing in construction is performed safely, efficiently, and with high-quality outcomes. Moreover, they provide essential guidance for the qualification of materials, processes, and personnel involved in additive manufacturing for construction, thereby supporting the advancement of this innovative technology.

2.1.3. Challenges in Medium-scale 3D Printing

In comparison to laboratory-scale 3D printing research, medium-scale 3D printed concrete (3DPC) is utilized for practical construction projects, including real-size elements, formworks, and monolithic buildings. Consequently, medium-scale 3DPC can be regarded as an advancement over lab-scale 3DPC. Furthermore, medium-scale 3DPC can be categorized

into three types: 1) 3D printing elements, 2) 3D printing formworks, and 3) on-site monolithic 3DPC, as illustrated in Figure 2.3. In this specific project, types 1 and 3. The process of 3D printing elements encompasses several stages, including the preparation and transportation of concrete, the fabrication of prefabricated elements in a controlled factory environment, the transportation of these elements to the construction site, and their subsequent assembly on-site (TotalKustom, 2019; Anton et al., 2021; Khoshnevis et al., 2006; Lim et al., 2011). Research on 3D printing formwork has been conducted both in factories and on-site (Xiao et al., 2021).

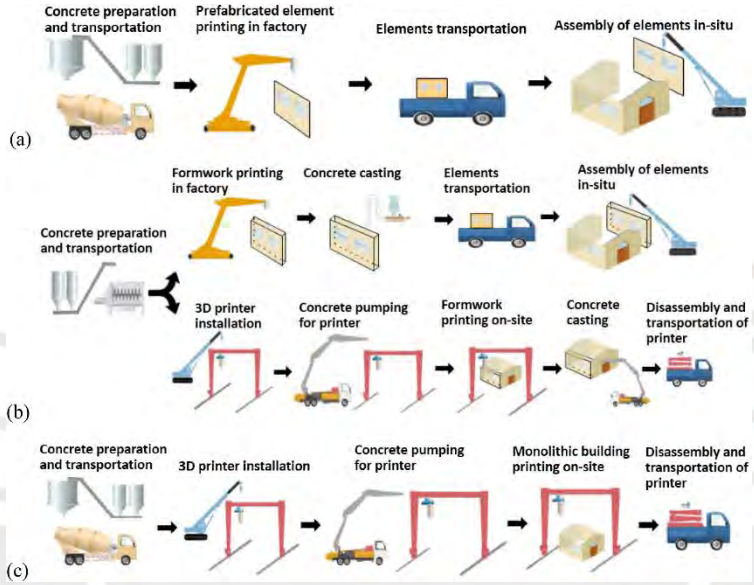

Figure 2.3. Types of medium-scale 3DPC: (a) printed elements, (b) printed formworks, and (c) on-site monolithic 3DPC (Xiao et al., 2021).

In current years, vast study has been done in laboratories to investigate the printability and mechanical properties of 3D printed concrete (3DPC) (Panda et al., 2019; Shakor et al., 2017; Figueiredo et al., 2020; Tay et al., 2019; Roussel, 2018). Additionally, numerous optimizations have been developing the enhancement of the mechanical properties of 3DPC, including improvements in interlayer strength through mesh reinforcement, the incorporation of fibers, and the use of admixtures (Marchment & Sanjayan, 2020; Bos et al., 2019; Nematollahi et al., 2018; Ding et al., 2020; Sikora et al, 2021; Panda et al., 2017).

Concurrently, the printability of 3DPC, encompassing aspects such as pumpability, extrudability, and buildability, has also been a focus of study and improvement in various

laboratories (Figueiredo et al., 2019; Tay et al., 2019; Kruger et al., 2019; Panda et al., 2019). To meet these specifications, the rheological properties of fresh printable concrete must differ from those of traditional concrete. Printable concrete should demonstrate high flowability and an extended setting time during storage, pumping, and extrusion. After deposition, it should exhibit low flowability, high green strength, and a rapid setting rate (Malaeb et al., 2015; Mechtcherine et al., 2019).

In addition to printability, the environmental and economic aspects of medium-scale 3D printed concrete (3DPC) are also significant areas of study. While the overall cost of construction using 3DPC technology is viable with traditional construction methods due to reduced labor expenses and the elimination of formwork, the price of printable concrete material remains higher than that of conventional concrete (Han et al., 2021). Lowering printing ink costs is crucial for reducing 3DPC project expenses. Various methods can boost economic and environmental characteristics, such as using geopolymer, supplementary cementitious materials, and printing hollow structures (Panda et al., 2017; Panda & Tan, 2018; McLellan et al., 2011). Additionally, incorporating coarse aggregates and recycled aggregates in 3D printing concrete reduces cement consumption, thereby decreasing carbon emissions and printing costs (Xiao et al., 2021).

It is essential to develop a concrete mix design that exhibits thixotropic rheological behavior and is resistant to segregation, while being pumpable, extrudable, buildable, and suitable for printing in various weather conditions. This mix should incorporate small coarse aggregates to ensure adequate mechanical properties and prevent clogs within the 3D printing equipment. Furthermore, the formulation should have appropriate tensile properties to minimize or eradicate the necessity for steel reinforcement. It is also essential to use locally available materials to avoid the necessity of acquiring products from overseas (Al-Tamimi et al., 2023).

In addition, the reinforcement construction and the 3D preparation and mix must be considered. Reinforcement construction is a critical area of study in both lab-scale and medium-scale 3D printed concrete (3DPC) to ensure structural strength and compliance with building standards (Asprone et al., 2018; Mechtcherine et al., 2018; Li et al., 2020; Bester et al., 2021). Various methods have been proposed, the most common method involves printing one layer of filament, placing horizontal reinforcement, and then printing the next layer,

repeating this process as needed (Xiao et al., 2021). Additionally, Bos et al. (2017) developed a 3DPC system capable of automatically and synchronously print filaments and place metal cables, significantly enhancing post-crack resistance. Although the bond strength of 3DPC with metal cables is lower than that of cast concrete with conventional ribbed rebar, this automated approach shows promise for medium-scale 3DPC constructions (Xiao et al., 2021).

Conversely, in medium-scale 3D printing, a greater volume of concrete must be produced and transported per unit of time to meet efficiency requirements. Mueller et al. (2017) proposed a method to store and transport dry and liquid mixture ingredients separately, ensuring proper particle size distribution during automated mixing and production. The necessity for concrete suitable for medium-scale 3D printing technology has been acknowledged (Mechtcherine et al., 2019). A list of the mix designs used with concrete for 3D printing is shown in Table 1.

Table 1. Mix proportions of concrete used in different research (Xiao et al., 2021)

Reference	Cement	Other binders	Micro silica	Fine aggregates	Coarse aggregates
Malaeb et al. (2015)	1	0	0	1.920	0
Weng et al. (2018)	1	1	0.1	0.5	0
Gosselin et al. (2016)	1	0.286	0.286	1.286	0
Le et al. (2012)	1	0.286	0.1	2.143	0
Ji et al. (2019)	1	0	0	3.2	3.620
Mechtcherine et al. (2019)	1	0.4	0.3	>3.369	<0.886

Researchers at Tongji University have devised a technique utilizing ready-mixed concrete with a maximum coarse aggregate size of 15 mm to fulfill production and transportation requirements (Ji et al., 2019). This ready-mixed concrete, which is produced at a mixing station, becomes suitable for 3D printing following secondary on-site mixing with additives. This method effectively addresses the production, transportation, and environmental challenges associated with medium-scale 3D concrete printing (Xiao et al., 2021).

2.2. Materials for 3D Printing in Construction

Concrete is a widely used construction material, and with advancements in printing technology, numerous rapidly built cement-based structures have emerged. Notable examples include a 400-square-foot home printed in Russia within 24 hours by ApisCor (Apis Cor, n.d.), a 400-square-meter, two-story villa constructed on-site in 45 days by Huashang Tengda (Scott, 2016), a bus stop in Shanghai, China, made from construction waste (CGTN, 2018), and the 95-square-meter Yhnova™ house, completed in 54 hours by Batiprint3D (Furet et al., 2019).

With the increasing emphasis on sustainability, there is a growing interest in environmentally friendly materials such as geopolymers and earth-based substances. Geopolymer-based products generally incorporate components like fly ash and slag derived from industrial waste (Xia & Sanjayan, 2016; Panda et al., 2017; Alves et al., 2021; Alves et al., 2022). Research has evaluated the printing capabilities of fly ash-based geopolymer (Panda et al., 2017). Additionally, Al-Qutaifi et al. (2018) investigated the constructability of fly ash-based mixtures. Another study by Panda et al. (2018) examined the effects of ground granulated blast-furnace slag (GGBS) and silica fume on the properties of fly ash-based printing mixtures.

Therefore, in search of more sustainable options, the idea of using the earth emerged. Earthen materials have a rich historical background. In the early 20th century, earth was replaced by modern industrial materials as a building material in Western countries (Rojat et al., 2020). However, earth is the first-born building material, its usage dates to around 10,000 BCE in Mesopotamia (Heathcote, 1995), and approximately 30% of the world's existing architecture is made of earth, with its territory spread presented in Figure 2.4.

Moreover, the advantages of earth-based materials include lower environmental impact (Aubert et al., 2016; Gomaa et al., 2022), ease of acquisition, and good thermal performance (Gomaa et al., 2022). Rammed earth is a simple and cost-effective technique to achieve high thermal mass in construction walls (Dobson, 2015). Combining additive manufacturing with earth-based materials could lead to a more sustainable building production

process, significantly impacting the future construction industry (Ji et al., 2023).

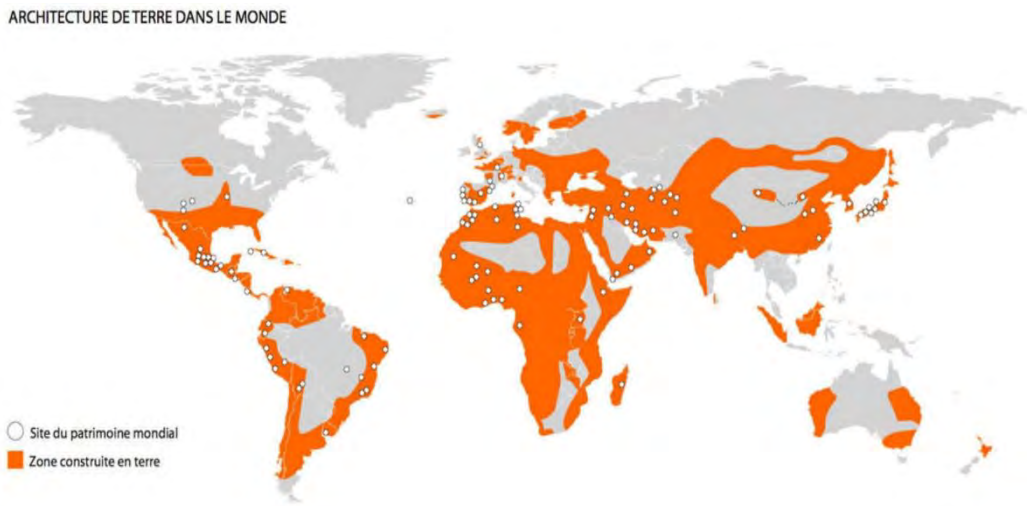

Figure 2.4. Earthen construction worldwide. (CRA Terre, 2021).

2.2.1. Earth-Based Mixtures: Applications and Benefits

In 2020, the construction sector accounted for 37% of global greenhouse gas emissions (REN21, 2022) and generated 25% of the world's solid waste (Fritz Benachio et al., 2020). Given the significant pollution associated with this sector, it is crucial to find maintainable methods and materials to mitigate its harmful impacts on both the environment and society (Faleschini et al., 2023).

Cesaretti et al. (2014) investigated the use of D-shape technology for constructing habitats with lunar soil in the context of using earth materials for 3D printing. A. Perrot et al. (2018), Veliz Reyes et al. (2018), and Alqenaee et al. (2022) examined the possibility of the usage of earth-based materials for extrusion in 3D printing. Despite some load-bearing challenges, the last year earth structures produced by WASP in Italy highlight the potential for earth-based residential construction as is shown in Figure 2.5.

Figure 2.5. 3D printed clay house (Mario Cucinella Architects, 2024)

Nevertheless, these studies remain in their preliminary stages. Bajpayee et al. (2020) illustrated the multi-scale approach for designing appropriate construction materials using soil for 3D printing, as shown in Figure 2.6. This figure delineates the design process from atomic-level considerations to macroscopic properties. This study seeks to initiate the first stage of characterizing and developing soil-based material for 3D printing while evaluating its performance in these applications.

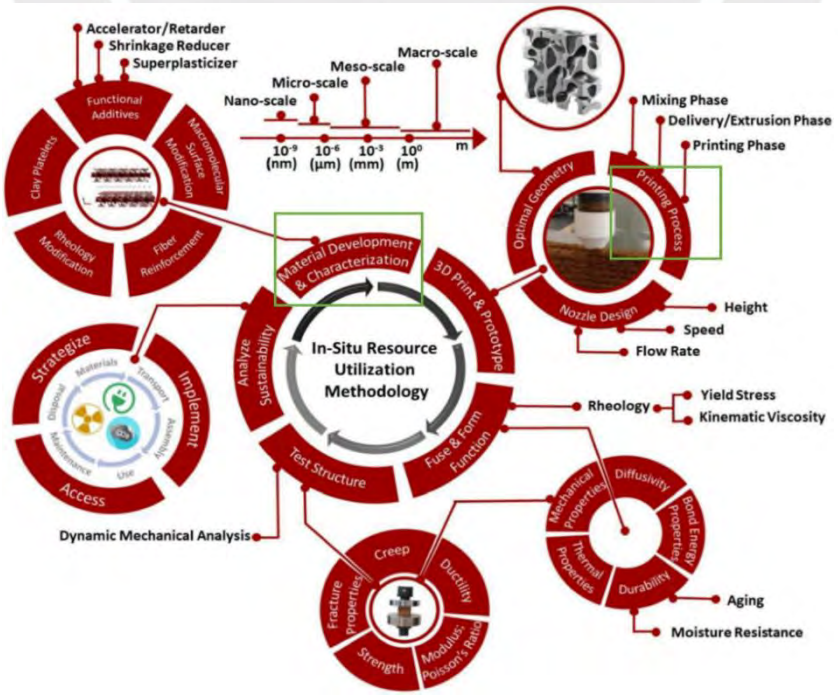

Figure 2.6. Process flow for soil utilization (Bajpayee et al., 2020)

Likewise, earthen material, sourced from natural soil, is abundant globally. It mainly comprises silica and limestone particles, along with a minor portion of fine micrometer-sized clay particles that function as the binder (Fabbri et al., 2022). Clays consist of sheets of aluminate and silicate with a strong attraction to water. Considering certain temperature and pressure conditions, clay particles either preserve water during drying or absorb it while dampening, forming capillary bridges that provide the material with mechanical endurance (Van Damme et al., 2010). Additionally, this water affinity endows earthen materials with hygrothermal regulation properties (Azil et al., 2023).

The carbon footprint of earthen structures constructed employing traditional methods such as rammed earth or cob is minimal due to the minimal transformation of the material and the reliance on human labor. (Pacheco-Torgal & Jalali, 2011; Assunção et al., 2024). Digitalizing earthen construction can reduce labor intensity and increase productivity, making it economically viable in first-world nations (Kloft et al., 2019; Schweiker et al., 2021). This method allows for mass production and standardization, tackling the lack of industrialization in earthen construction globally (Sonebi et al., 2022; Hebel & Heisel, 2017).

2.2.2. Fiber Reinforcement in Construction Mixtures

Controlling rheological parameters is key to achieving printable capacity and vertical constructability in cement-based materials. Firstly, it is essential to adjust shear yield stress and cohesion to ensure printability (Varela et al., 2024). Over time, structural build-up needs to increase to prevent the printing piece from experiencing a plastic collapse, thoroughly developed by Varela et al. (2023a), Roussel (2018), and Wolf et al. (2019). Adding fibers in 3D printing mortars can effectively attend these challenges, as suggested by Li et al. (2024) and Varela et al. (2023b).

Specifically, plant fibers present a promising prospect due to their strengthening capabilities and their natural, renewable origins, as noted by Fidelis et al. (2013), Varela et al. (2023b), and Bohuchval et al. (2020). The unique characteristics of Sisal fiber (SF), such as its irregular cross-section, high flexibility, strength, and water absorption capacity, improving the shrinkage highlighted by Toledo Filho et al. (2009), De Andrade Silva et al. (2008), Ren et al. (2022), and Castoldi et al. (2024), make it an excellent choice for reinforcing printable

mortars. These properties can enhance both the rheology and the hardened properties of the material. For a better choice of fibers, it is worth first prioritizing the ones that have a lower CO_2 footprint, hence proving their sustainability. Table 2 shows the available fiber options.

Table 2. CO_2 footprints of natural fiber, synthetic fiber, and polymer matrix material (Shahinur & Hasan, 2019).

	Fiber	**CO_2 footprint (kg-CO_2/kg)**	**References**
Natural fiber	Jute	0.566	(Singh et al., 2018)
	Coir	0.367	(Grasselly et al., 2009)
	Flax	0.520	(Singh et al., 2018)
Synthetic fiber	Glass	0.85	(Patty & Anne, 2004)
	Glass fiber	1.45	(Anon, 2012)
	Glass composite	8.1	(Shahinur & Hasan, 2019)
Polymer materials	Polyester	0.00952	(Patty & Anne, 2004)
	PP	1.4	(Narita et al., 2002)
	PE	1.3	(Narita et al., 2002)
	Epoxy	5.7	(Anon, 2012)
	PLA	4.7 ± 1.5	(Patty & Anne, 2004)

The study of Shahinur & Hasan made a comparison among natural, synthetic, and polymer fibers, which were included here for referential purposes. However, this will be only considered for the discussion of natural fiber since it is the target of this thesis study. Moreover, despite the sisal fibers not appear in Table 2, a study from Broeren et al (2017) gave the average number of 0.75 CO2 footprint (kg-CO2/kg), so it will be still considered in further study. Furthermore, the mechanical properties of some natural fibers are displayed in Table 3 where the best options overall are jute, bamboo, and banana fibers. Therefore, there will be a predilection towards the jute fibers considering their affordability and easier process to manipulate.

Table 3. Mechanical properties of natural and synthetic fibers. (Shahinur & Hasan,

2019).

Fiber	Density (gm/cc)	Tensile strength (MPa)	Young's modulus (GPa)	References
Sisal	1.45 – 1.50	67	3.7	(Célino et al., 2014)
Flax	1.54	28 - 85	0.3 - 2	(Célino et al., 2014)
Coir	0.67 – 1.15	220	6	(Célino et al., 2014)
Jute	1.30 - 1.45	393 – 773	13 – 27	(Célino et al., 2014)
Bamboo	1.32	140 – 230	11 – 17	(Célino et al., 2014)
Banana	1.35	335	33.8	(Célino et al., 2014)

The addition of sisal fibers in concrete marginally decreases compressive strength at higher percentages but enhances overall structural performance. It is advised to use 5 cm long fibers in quantities of 0.5% to 0.75% by weight (Sosa et al., n.d.). Synthetic fibers, especially polypropylene (PP) fibers, have been used for many years to reduce or prevent plastic shrinkage cracks in concrete. Dahl (1986) observed a notable decrease in cracking by incorporating fibrillated polypropylene fibers at a concentration of 1 kg/m³ of concrete. These fibers were added in packs during the blending process.

Therefore, given that concrete production depletes substantial quantities of non-renewable resources and contributes significantly to CO_2 footprint, substituting synthetic fibers with renewable ones, especially vegetable fibers, is a step towards sustainability (Torgal & Jalali, 2011). Soroushian and Ravanbakhsh (1998) successfully utilized cellulose fibers at a dosage of 0.06% by volume to reduce plastic shrinkage cracking in both normal and high-performance concrete. Soroushian (2000) further reported that incorporating 0.2% cellulose fibers by volume significantly reduced the maximum crack width in concrete, decreasing it from approximately 0.14 mm to 0.02 mm.

Conversely, Boghossian and Wegner (2008) carried out an experimental study on mortars reinforced with flax fibers, concluding that natural fibers were equally effective as PVA fibers in mitigating both the number of cracks and the overall crack area. The primary

conclusion of this study indicates that both kenaf and jute fibers are viable alternatives to polypropylene (PP) fibers for mitigating plastic shrinkage cracking in concrete, as well as other fresh cementitious materials such as mortars and renders (Lura et al., 2024).

2.2.3. Properties and Optimization of Earth Mixtures

Research shows unstabilized rammed earth and compressed earth blocks can be sustainable alternatives to concrete caused by their low embodied carbon. These methods can reduce carbon impact by approximately 80% when used as nonstructural building elements (Hammond & Jones, 2008). In addition to their environmental benefits, these materials offer excellent thermal performance. For instance, Shibam, Yemen, features load-bearing earth structures as tall as 10 stories, demonstrating the strength and durability of these materials. Studies have shown that unstabilized raw earth-building elements can achieve compressive strengths between 1.5 and 4 MPa (Giuffrida et al., 2019). Nevertheless, the extensive acceptance of structural building codes for earthen manufacture remains a challenge in most countries (Curth et al., 2024).

Subsequent to this, during the preparation of soil for construction purposes, the material must be thoroughly sifted, and water should be added to obtain a consistency suitable for pumping (Curth et al., 2024). Accurate water content measurement involves determining the soil's initial water content by weighing a sample before and after oven drying, as specified in ASTM D2216. Additionally, the water content for 3D printing earthen mixes must be higher than that used for compressed earth blocks (CEB) or rammed earth to aid in the pumping process. This increased water content leads to extruded materials generally having a higher density than traditional earthen methods. Balancing shrinkage rate with desired final material density is crucial (Curth et al., 2024).

Furthermore, the initial evaluation of soil suitability can rely on straightforward field tests provided by organizations like the Food and Agriculture Organization of the UN and CraTerre. These practical methods, including dampening the soil to assess its texture, conducting drop tests, and performing ribbon tests to evaluate clay content and cohesiveness, offer a cost-effective starting point (Centre for the Development of Industry & CraTerre-EAG, 1998; Food and Agriculture Organization of the United Nations, n.d.). However, for more comprehensive assessments, geotechnical, structural, and chemical laboratory analyses can

complement on-site evaluations. In many cases, though, physical soil analysis conducted on-site is sufficient to initiate construction work.

2.3. Fresh-State and Hardened-State Properties

The materials used in the 3D printing process must meet the printability requirements of the extrusion printing system, including open time, interlayer bonding, buildability, pumpability, extrudability, among others (Ji et al., 2023). Among these factors, pumpability and extrudability are essential for ensuring the material can be efficiently transferred and printed, producing a continuous and well-defined filament at the start of the process (Ji et al., 2023). Pumpability refers to the ease with which a material can be transported through the system, while extrudability defines the ability of the fresh mix to pass smoothly through the nozzle without clogging. Buildability represents the material's capacity to sustain layered construction, while open time indicates the period after which the material begins to lose its extrudability (Choi et al., 2014).

Extrudability is the capacity of a material to be consistently passed through an extrusion system, whereas buildability refers to its ability to retain its extruded form under the load of consecutive layers. In the current study, the extrudability was evaluated through qualitative observation of the mixture's flow during the printing process (Carcassi et al., 2024). The buildability assessment was conducted quantitatively by counting the number of vertically deposited layers, up to a maximum of five consecutive layers. This evaluation included examining the bond between layers, the form preservation of the freshly extruded specimens, and the stability of the built layers in terms of their potential to fail (Carcassi et al., 2024).

Currently, researchers are concentrating on the fundamental mechanical properties of 3D printed concrete after it hardens, particularly its strength and the consequences of printing parameters and processes on the mechanical strength of printed components (Cui et al., 2024). The raw materials are vital for the successful printing of components. Mineral admixtures serve as a key factor in the printing mixture, significantly influencing the working performance and enhancing both early and late strength in printed concrete. However, there is limited research on how mineral admixtures currently affect the mechanical properties of printed concrete (Cui et al., 2024).

Compressive strength refers to the capability of a material or structure to withstand loads. The ultimate compressive strength is the highest uniaxial stress a material can withstand before failure. The mentioned strength is commonly established experimentally through a compressive test, applying an uniaxial compressive load until the material fails (Siddique & Mehta, 2014). There are many other tests in hardened-state whose purpose is to evaluate and examine the impermeability of the 3D printed samples; however, they will be discussed thoroughly in the durability section.

2.4. Durability in 3D Construction Printing study

Concrete durability is defined as its aptitude to resist distinctive categories of degradation, such as weathering, chemical attacks, and abrasion, over its intended service life (American Concrete Institute, 2018). Porosity and pore morphology are key factors influencing durability, as they significantly affect mechanical properties (Sun et al., 2022; Yu et al., 2021; Ma et al., 2022; Chen et al., 2020; Geng et al., 2020; Sikora et al., 2021) and durability performance (Sun et al., 2022; Zhang et al., 2021; Rui et al., 2023; Babafemi et al., 2022; Han et al., 2022) of 3D printed concrete (3DPC). Moreover, the penetrability of the concrete pore system is particularly critical in harsh environments, as highlighted in ASTM C1585 (2020).

Building on this, the durability characteristics of 3DPC extend across a wide range of performance metrics, including creep, shrinkage, fire resistance, freeze-thaw resistance, acid and sulfate resistance, carbonation resistance, and resistance to chloride access (Ler et al., 2024). Water absorption testing is crucial for assessing durability, as it indirectly measures the concrete's water-accessible porosity. In fact, three out of four durability tests in the present study involve water absorption to estimate porosity, underscoring its importance in assessing the material's overall performance

In addition, a review of existing studies reveals that shrinkage tests are the most examined durability assessments, with 28 studies focusing on this aspect. Following this, researchers have conducted 15 studies on chloride ingress, 14 on freeze-thaw resistance, 11

on fire resistance, and 10 on carbonation. Conversely, fewer studies have addressed creep (5), sulfate attack (4), and acid resistance (2), as shown in Figure 2.7. It is worth emphasizing that this review exclusively covers extrusion-based 3D concrete printing (3DCP) and does not include studies on the selective binding method, such as particle-bed-based or powder-based techniques (Ler et al., 2024).

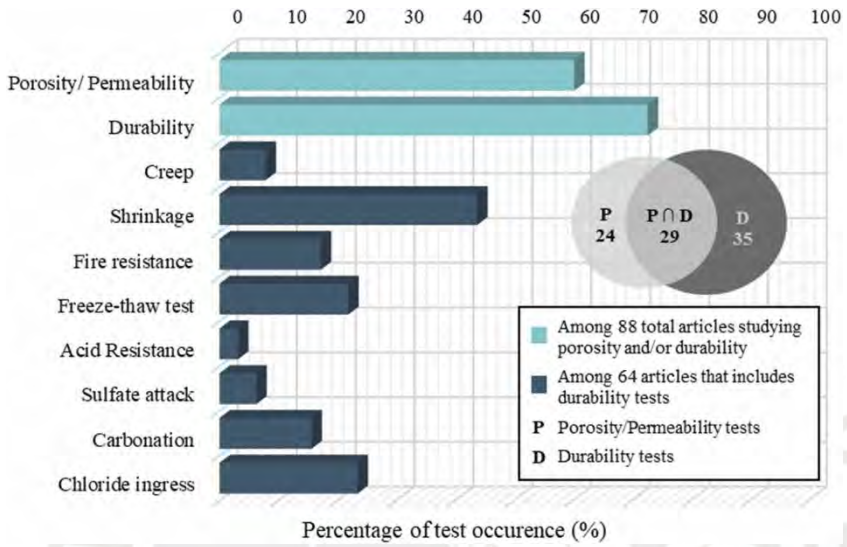

Figure 2.7. Porosity and permeability, as well as durability tests frequency (Ler et al., 2024).

Chapter III

Methodology

3.1. Materials

This segment outlines the materials employed in this study: soil, cement, water, and jute fibers, which are essential components of the experimental setup.

3.1.1. Soil

The soil sample was collected from a quarry in Carabayllo district, Lima, Peru. To prevent potential nozzle blockage, the soil underwent sieving using the N°20 (0.85 mm) from ASTM standards. Following the sieving, various physical characterization examinations were directed on the earth, adhering to ASTM guidelines such as ASTM D6913 (2021): Standard Test Methods for Particle-Size Distribution (Gradation) of Soils Using Sieve Analysis, ASTM D792 (2020): Standard Test Methods for Density and Specific Gravity (Relative Density) of Plastics by Displacement, ASTM D4318 (2018): Standard Test Methods for Liquid Limit, Plastic Limit, and Plasticity Index of Soils, ASTM D854 (2023): Standard Test Methods for Specific Gravity of Soil Solids by the Water Displacement Method, and ASTM D2216 (2019): Standard Test Methods for Laboratory Determination of Water (Moisture) Content of Soil and Rock by Mass. The particle-size distribution curves resulting from the sieving process revealed that the soil consists of 4% medium sand by weight, 30% fine sand content, 41% silt-

sized particles, and 25% clay content. These percentages are determined based on the particle size range acclaimed by the Unified Soil Classification System (USCS). Additionally, the soil classification highlights its potential as an extrudable and printable material, primarily comprised of fine clayey particles with low plasticity. This composition ensures pumpability (Perrot et al., 2018).

3.1.2. Cement

Ordinary Portland Cement (OPC) is a finely ground substance created through the intergrinding of gypsum and clinker. Clinker, constituting the major portion of cement at approximately 95%, is a hydraulic material produced through pyro-processing. It primarily comprises tricalcium silicate (C_3S), dicalcium silicate (C_2S), tricalcium aluminate (C_3A), and tetra calcium aluminate (C_4AF). This study used Portland Cement SOL type I (UNACEM) to chemically stabilize the soil matrix.

3.1.3. Water

Drinkable water was employed to organize the control soil-cement matrices. The potable water temperature was recorded at 20 °C. Additionally, it is remarkable to notice the difference between the theoretical and actual water quantities for a proper comparison and evaluation of the mixed proportions. Further discussion on this matter will be provided in the section on Humidity Control for Weathering.

3.1.4. Jute Fibers

Jute is obtained from the bark of the white jute plant and, to a lesser degree, from jute mallow, both of which thrive in tropical regions. It is among the most affordable and widely accessible natural fibers (Song et al., 2021; Ali et al., 2015; Food and Agriculture Organization of the United Nations, n.d.)., presenting a variety of advantageous characteristics such as considerable tensile strength (ranging from 215 to 800 MPa), low density (730–1500 kg/m3), and reduced thermal conductivity (Rangasamy et al., 2021; Khan et al., 2015; Majumder et al., 2022; Bui et al., 2022). Found in its regular state, jute is a rapidly extending herbaceous shrub classified under the genus Corchorus within the Malvaceae family (Shukla & Mittal, 2022). The largest widespread species of jute is grown for commercial production in India, Bangladesh, China, and Thailand (Hejazi et al., 2012). The incorporation of jute fibers will be undertaken to assess their impact on the various properties outlined herein. In the current

paper, the quantity of fibers used is 0.3% of solids weight.

3.2. Experimental plan

The 3D printing system, named *Colibrí* (Hummingbird in English), was utilized for all printing experiments. This prototype, developed at PUCP (NZS D4298, 2020), is a small-scale gantry-type 3D printer. It possesses a printing volume of 1 x 1 x 1 m, with printing rates varying from 15 to 150 mm/s, and a flow rate range of 1.5 to 8.5 L/min. The flow rate is manually adjustable in a MAI PICTOR concrete pump, through a mechanical inverter.

3.2.1. Mix design and material preparation

3D printed samples manufacturing procedure comprises of three phases: i) material preparation, ii) extrusion, and iii) deposition. During the stage that material is prepared, the base soil and OPC were only dry-mixed, followed by the addition of water to the solid component. The mixing process occurred at 450 rpm using a mortar mixer equipped with a 120 mm-diameter paddle, and it continued until a uniform mixture was achieved, which typically took around 10 minutes. During the extrusion phase, the soil-based mixture was transferred into a mortar pump after the hydraulic hose had been lubricated.

The pump's velocity was adjusted to level 2/10, enabling a material flow rate ranging from 0.56 to 0.97 L/min, conditioned by the material's flowability. To maintain constant extrusion, an easy push was necessary during the pouring of the material. Once a constant flow of material was established from the nozzle, the deposition process commenced. The 3D printer prototype was equipped with an SD memory card, which contained the specified instructions in the G-code. As a result, the printer head relocated precisely corresponding to these instructions during the deposition phase.

3.2.2. Humidity control for weathering

Environmental conditions, especially humidity, have a substantial influence on the longevity and functioning of structures and materials. With an average humidity of 4%, representing a 2% increase in water content, as shown in Table 1. Understanding the dynamics of humidity and its fluctuations throughout the year is essential for maintaining the durability of construction projects and preserving the integrity of various materials. The district of San

Miguel, located near the sea, experiences two distinct seasons that influence humidity levels, which can reach 100% (SENHAMI, 2023). Each dose of water will be classified into 3 groups of OPC content 5, 10, and 15%. Likewise, they will study mixed designs with and without fibers, the content is distributed in Table 4.

Table 4. Distribution of mix-designs considering the effect of humidity.

Stage	Matrix ID	Added water content (% by weight of water in the matrix)	Water content (% by weight of water in the matrix)	OPC content (% by weight of OPC mixed in the solids)	Fiber content (% by solids weight)
Mix-design and validation of soil-cement mixtures	SC26	24	26	5, 10, 15	0
	SC27	25	27	5, 10, 15	0
	SC28	26	28	5, 10, 15	0
Mix-design and validation of fiber-reinforced soil-cement mixtures	SCF26	24	26	5, 10, 15	0.3
	SCF27	25	27	5, 10, 15	0.3
	SCF28	26	28	5, 10, 15	0.3

3.2.3. Procedure

The distribution for analyzing the fresh and hardened-state properties from a 3D printing's mix-design, in this paper will be in 5 stages, as displayed in Figure 3.1a) and b). Stage 1 will explain the necessary printing parameters such as the print speed which is edited in G-code and the speed that the extruder pump exerts. The correct calibration of these 2 parameters will have a strong impact on the print quality and the study of other properties such as stacking and shrinkage cracking. Likewise, based on these first results, only a single ideal water content will be evaluated, with the 3 OPC contents. Stage 2, on the other hand, will be the section that will be studied most extensively, and will be studied fresh-state and hardened-state properties. In the case of fresh-state properties, include the shear stress, over-time shear stress, and Vicat test; while among the hardened-state properties, there is the compression test that provides elastic modulus results, as well. Stage 3 is executed as a medium-scale impression in which are only used the parameters and mix-design that had the best results. This impression after 7 days is observed to crack, so this cracking is measured and dosages with and without added fibers are studied, in stage 4. Finally, in stage 5, the shrinking cracking

analysis with fiber-reinforced medium-scale printing.

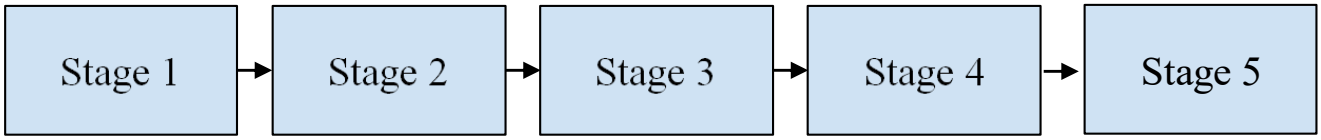

a)

Stage 1 - Definition of printing parameters for non-reinforced and reinforced soil-cement matrices
Stage 2 - Fresh and hardened state characterization of non-reinforced and reinforced soil-cement matrices
Stage 3 - Medium-scale earthen 3D printing
Stage 4 - Shrinkage cracking analysis
Stage 5 - Reinforced medium-scale earthen 3D printing

b)

Figure 3.1. a) Order and quantity of steps and b) the name for each one.

3.2.4. Fresh-state analysis

3.2.4.1. Filament printing test

This experiment is conducted to study the use of soil-cement mixtures. Further analysis was conducted to determine appropriate widths and heights based on different printing speeds. First, some tests were done as the 3D printer calibration process involved two key aspects: printing speed calibration and layer height calibration. The printer was tested using a simple soil mixture with a liquid content of 22%, considering the effects of humidity. Further analysis was conducted to determine appropriate widths and heights based on different printing speeds to accommodate soil-cement and soil-cement-fiber mixtures. The dimensions, geometry and other parameters are shown in Figure 3.2.

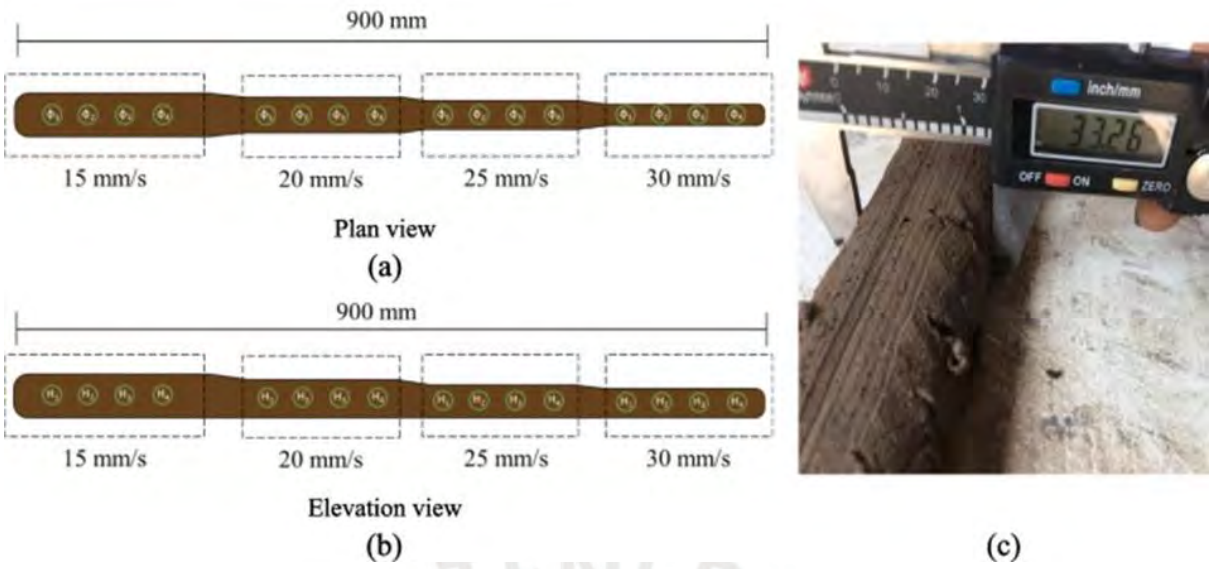

Figure 3.2. Filament printing experiments with earthen-based matrices.: (a) top-down view, (b) lateral perspective with marked measurement locations on the printed filaments, and (c) the procedure for measuring filament dimensions (Silva et al., 2022).

3.2.4.2. Shear vane test

The shear vane examination is crucial in evaluating a material or soil's shear strength and stability. By subjecting the sample to controlled shear stress, this test allows for determining its resistance to deformation and failure under applied forces. Understanding the shear strength characteristics of a material or soil is vital in various engineering applications, such as construction, geotechnical engineering, and foundation design. The shear vane test provides significant data concerning the material's behavior and ability to withstand shear forces. This protocol was based on the ASTM D2573 (2015). Therefore, the experiment will be executed for 6 minutes, with the vane in the first horizontal 180° position and rotating clockwise for 1 minute per quadrant. Once the time is finished, the vane is released and the measure the vane shows will be multiplied by 0.625 for having the result in kPa. The parts of the equipment are explained in Figure 3.3.

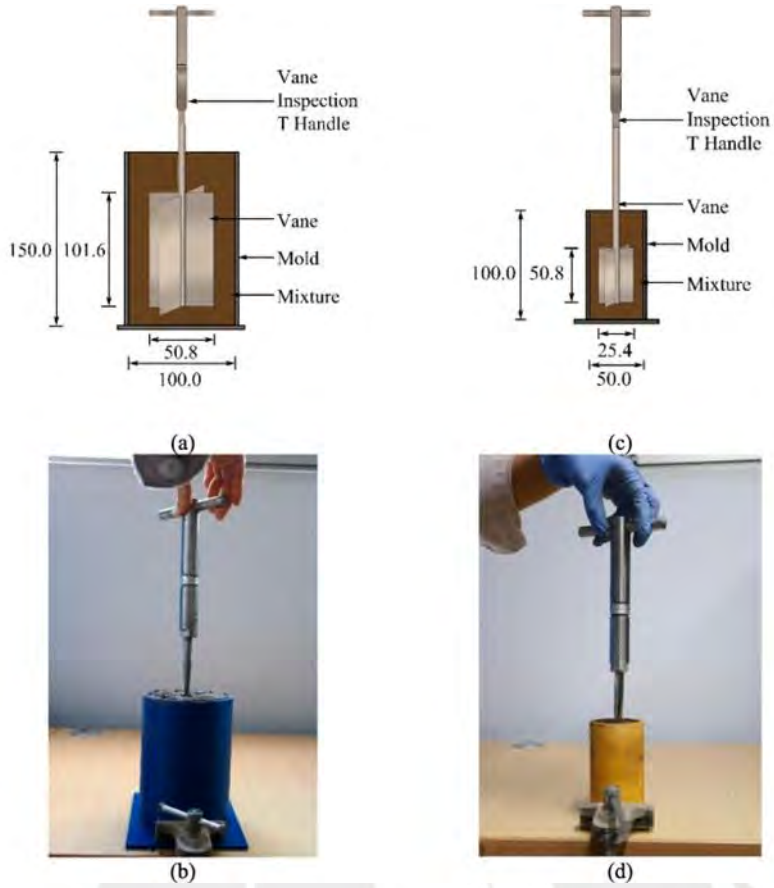

Figure 3.3. Shear vane experiments: (a) Vane and its housing sized at 50.8 × 101.6 mm, (b) Photograph depicting the actual test employing a 50.8 × 101.6 mm vane, (c) Vane and its container sized at 25.4 × 50.8 mm, and (d) Actual photograph of the tests utilizing a 25.4 × 50.8 mm vane. Measurements are in millimeters (mm) (Silva et al., 2022).

3.2.4.3. Overtime shear vane test

In this section, an overtime test was conducted using the shear vane test. The overtime refers to the duration a sample remains workable and extrudable, typically 25 to 30 minutes, depending on room temperature and humidity. So, in this experiment, the shear stress of each mix-design will be measured at 0, 10, 20, 30, 60, 90, and 120 minutes, so it can be studied its workability, which impacts the extrudability and printability.

3.2.4.4. Vicat-Penetration Resistance Test

A Vicat test was conducted, a method used to verify the setting time and early strength development of cementitious materials, based on the protocol of ASTM C191 (2015). The test involves measuring the penetration resistance of a Vicat needle, the Vicat equipment shown in Figure 3.4, into the material in the black container as it undergoes the setting process. The

Vicat test is essential in assessing the quality and functioning of cement-based materials. It provides valuable information about the material solidification speed and adds strength, which is crucial for various applications such as construction, concrete production, and quality control.

Figure 3.4. Vicat equipment of the UTEST brand was very similar to the one used for the tests in this section (UTEST, 2023).

3.2.4.5. Rheological characterization

The rheological characterization focused exclusively on evaluating the material's thixotropy. To perform this characterization, an Anton Paar Smart Pave 92 Rheometer, supplied with a ball-type spindle, was used, as presented in Figure 3.5.a).

According to Figure 3.5.b), the protocol was centered around calculating the area between the loading and unloading curves and studying the unloading trending linear equation. These curves, shown in the diagram, represent the increase and decrease in shear rate, and the area between them reflects the thixotropic behavior of the material (Zhang et al., 2019). The larger the area, the more pronounced the thixotropy, indicating how the material's structure changes under shear stress and its ability to recover when the stress is reduced. The slope of the equation of the trending unload determines the plastic viscosity and its y-intercept represents the yield stress.

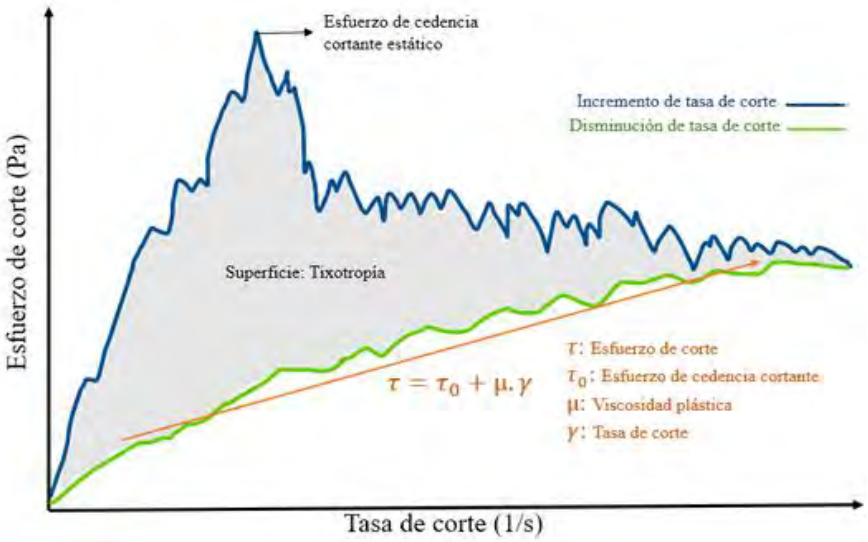

a) b)

Figure 3.5. Rheological test. a) Anton Paar Smart Pave 92 Rheometer is equipped with a ball-type spindle (Tudela Laura, 2024). b) Thixotropy test protocol (Tudela Laura, 2024).

3.2.5. Hardened-state analysis

3.2.5.1. Shrinkage analysis

Cracking refers to forming fractures or fissures in a material, compromising its structural integrity, and often resulting from excessive stress or inadequate material properties. Within the framework of 3D printing, acknowledging, and addressing cracking is fundamental for guaranteeing the quality and durability of printed structures. The procedure consisted of measuring with a graphic on a scale 1:1 shown in Figure 3.6. and comparing the cracks with which the measurement fits better. The analysis was evaluated since it was seen that the mixture that was not reinforced cracked after 7 days. While the one with fiber cracked after 28 days. Therefore, the 2 best dosages with and without fibers were studied in small walls of 40 cm long and 6 filaments stacked vertically.

Figure 3.6. This fissurometer was used to measure crack widths.

3.2.5.2. Compressive strength test at the ages of 7, 21, and 28 days

The compression test monitored the early-age mechanical strength development of soil-cement (SC) matrices to analyze the effect of mixture content and concentration on the compression strength of the matrices. Uniaxial compression tests were conducted at 3, 7, and 28 days on printed filament samples with a slenderness ratio of 2:1. The experiments were performed using the machine shown in Figure 3.7 at the same speed of 10 mm/s. The tested samples consisted of a soil-cement mixture with 5% cement by weight of solids (SC27 (5%)), and two other samples were earth matrices stabilized with cement at concentrations of 10% (SC27 (10%)) and 15% (SC27 (15%)) by weight of total solids.

Figure 3.7. Exceed® electromechanical test systems also known as the universal machine from the MTS brand (MTS, 2023).

3.2.5.3. Contact-angle test

The permeability of stabilized and unstabilized soil mixtures was evaluated using water contact angle tests. These samples were prepared by compacting them into three layers using a tamper and filling them with the mixture in the Vicat mold. After 28 days of curing at room temperature, the specimens were dried at 60°C for 2 days and then re-cured at room temperature until the change in mass did not exceed 0.2%. A single drop of distilled water (0.5 mL) was applied to the specimen surface, and the contact angle was measured using a Ramé-hart contact angle goniometer after 0, 60, and 120 seconds. The test arrangement is displayed in Figure 3.8. Finally, the soil mixtures were classified as hydrophobic (low permeability) if the contact angle was greater than 90°, otherwise, they were considered hydrophilic (high permeability). The contact angle tests were performed in the printable soil mixtures stabilized with SC27 (5%) and SC27 (10%).

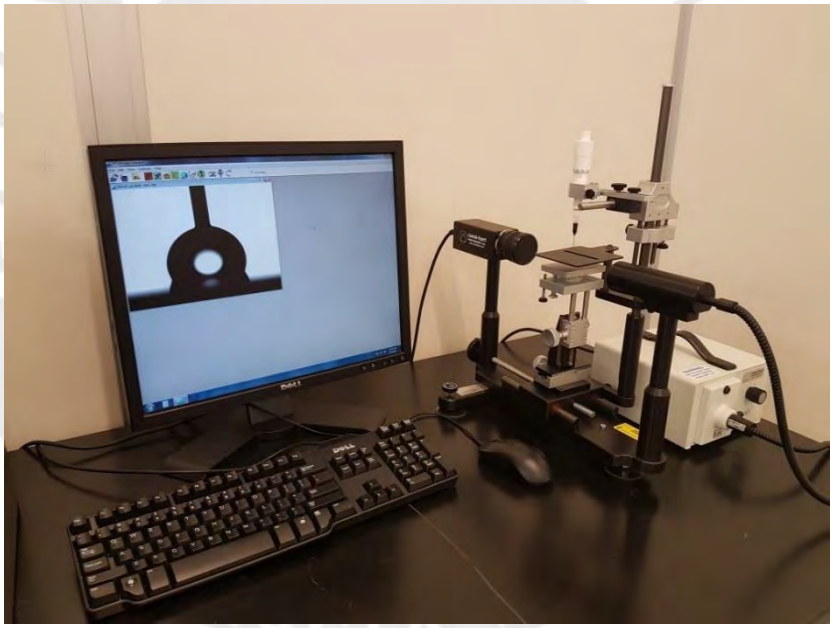

Figure 3.8. Contact Angle Goniometer (Ramé-Hart 200) (The Sara and Moshe Zisapel Nanoelectronics Center, 2017).

3.2.6. Durability tests

3.2.6.1. Immersion test

The immersion tests conducted aimed to evaluate the performance of the samples when exposed to water. The samples were immersed in water for a specified duration, and any weight changes were recorded. The low weight loss observed indicates the samples' ability to resist water absorption, highlighting their potential for enhanced durability and stability in

water-exposed conditions.

3.2.6.2. Absorption capacity

The water absorption capacity of the matrices was monitored to determine the pore size of the absorbent material. This was feasible because the mixtures exhibited a material loss of less than 2% by weight, which is considered an insignificant loss. The procedure followed is a modification based on ASTM C67, and the specimens were cured under laboratory conditions for 28 days before the test. The samples were then sunk in potable water for 24 hours. Quantities were recorded at regular periods: during the first 10 minutes, measurements were taken every 2 minutes due to the rapid water uptake, then every 15 minutes until 1 hour of immersion was reached. For the remaining hours, as the absorption rate slowed, measurements were recorded every 8 hours. The total water absorption capacity was estimated as the ratio of the variance between the saturated weight (Ws) of the specimen (after immersion) and the dry weight (Wd) of the sample (before immersion) to the dry weight, expressed as a percentage.

3.2.6.3. Accelerated erosion test

This study evaluated water erosion damage on 28-day-old 3D-printed earth specimens. A severe precipitation event was simulated using accelerated erosion tests with a rainfall intensity of 50 mm per 50 years, conducted for one hour. The accelerated erosion test mimics two sources of erosion during rainfall: wetting caused by increased water content in the specimen, triggering a decrease in internal cohesion, and the impact energy of water on the specimen, weakening or breaking already fragile cohesion bonds (Morel et al., 2012) as shown in Figure 3.9.a).

This examination was managed following the protocol of the NZS 4298 standard (1998). The test involves spraying water at a pressure of 150 kPa onto the surface of the 3D-printed sample positioned at 300 mm for 60 minutes or until the sample reaches considerable damage as presented in Figure 3.9.b).

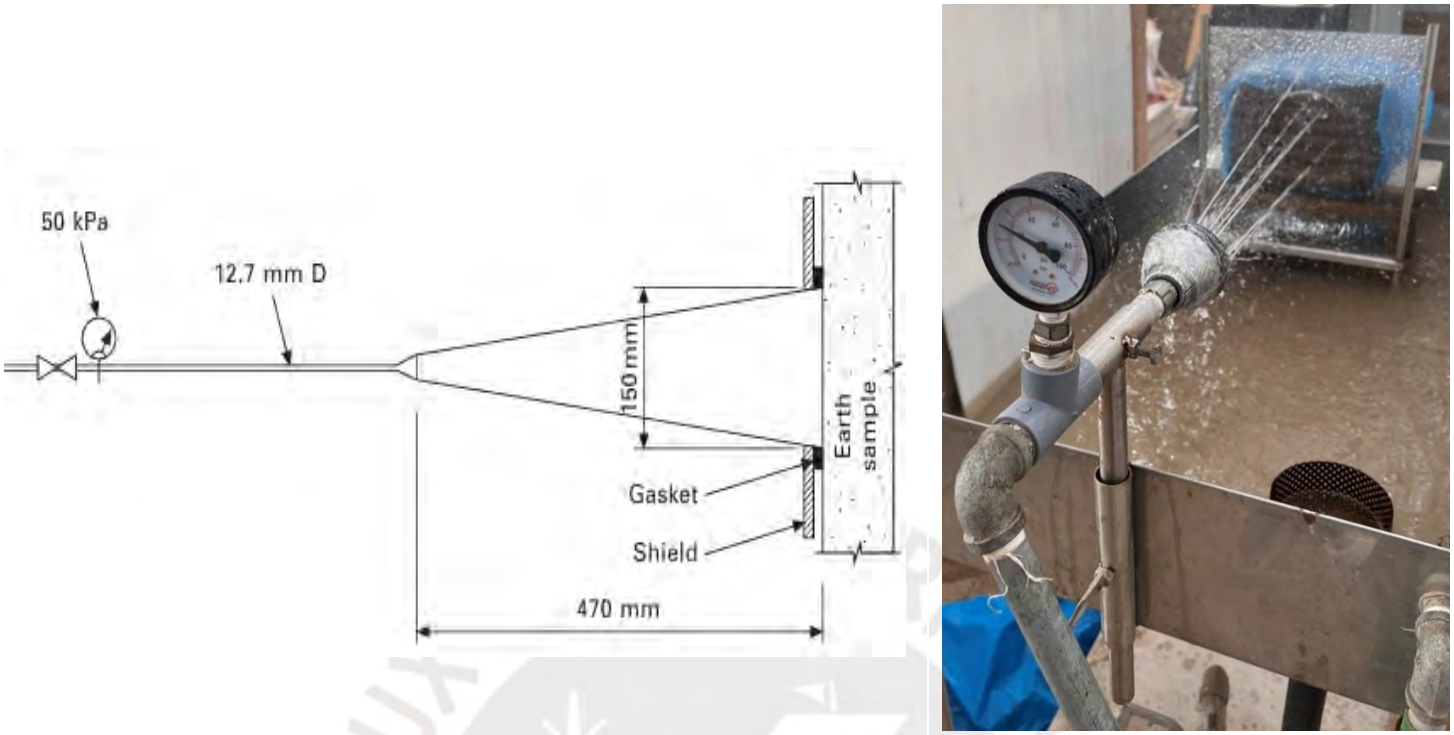

a) b)

Figure 3.9. a) Spray test, following Walker et al. (2005) b) Accelerated erosion test set-up.

Chapter IV

Analysis and result discussion

4.1. Stage 1: Definition of printing parameters for non-reinforced soil-cement matrices

4.1.1. Printing speed test

The printing speeds tested were 15 mm/s, 20 mm/s, 25 mm/s, and 30 mm/s, with water content percentages of 26%, 27%, and 28%. Additionally, each experiment was performed using three concentrations of cement: 5%, 10%, and 15% by weight relative to the total weight of solids. The primary objective of these experiments was to identify optimal printing parameters for soil-cement mixtures, considering the desired performance and structural characteristics. Figure 4.1 presents the findings of filament printing experiments on soil-cement matrices conducted at speeds of 15, 20, 25, and 30 mm/s.

As anticipated, the results demonstrated a significant influence of printing speed on filament width and height, with higher speeds leading to reduced filament dimensions. Likewise, water content showed a direct correlation with filament dimensions, as increased water content enhances the flowability of soil-cement matrices. While both printing speed and water content impact filament height and width, the latter has the most pronounced effect. Based on these findings, the lowest printing speed of 15 mm/s was chosen, as it produced thicker filaments, ensuring a sufficient contact area for the upper layers during stacking.

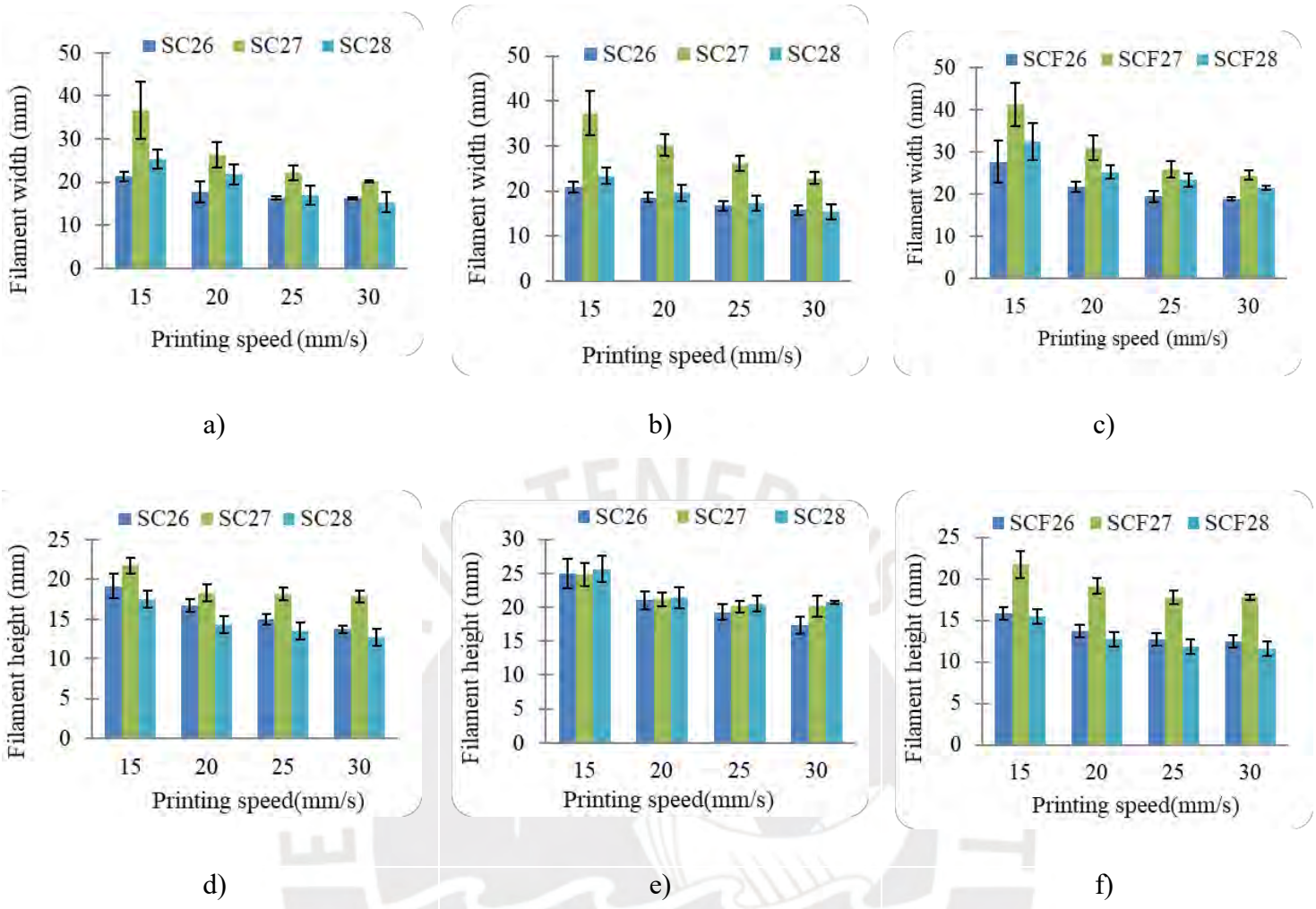

Figure 4.1. Variations in water content and printing speed widths of matrix prepared with a) 5%, b) 10%, and c) 15% OPC content and heights in d) 5%, e) 10%, and f) 15% of OPC content.

4.1.2. Stacking test

The stacking test is a mechanical test performed to assess the capacity of a material or structure to tolerate vertical loads or forces when stacked or piled. It involves stacking multiple layers or units of the material and evaluating their stability, resistance to deformation, and overall structural integrity. The stacking test is essential in various fields, such as construction, engineering, and manufacturing. It delivers significant understandings into the behavior and performance of materials under load-bearing conditions, particularly when subjected to vertical stacking forces. This test helps determine the suitability and durability of materials for stacking applications, such as building structures, load-bearing walls, or stacked product packaging.

The assessments were did using a velocity of 15 mm/s and a cement content of 15%, as these were expected to yield higher values and consequently provide more excellent stability. SC26 exhibited the poorest performance in the stacking tests, as shown in Figure 4.2. a), which can be attributed to the width of the printed filaments, which measured 21.5 mm. This width may have negatively affected the stability and load-bearing capacity of the stacked layers.

Nevertheless, SC27 and SC28, as presented in Figures 4.2, b), and c), proven the best performance in the stacking tests. The filaments in the matrix of SC27 and SC28 had similar dimensions, slightly exceeding 25 mm. This slightly larger size favored their construction capabilities and contributed to their overall stability and resistance to deformation under the stacking forces.

Nevertheless, it is worth mentioning that the bottom layer of the tower printed with SC28 underwent considerable deformation due to its high-water content. Suggesting that the high-water content negatively affected the structural stability of the printed tower, leading to deformations in the lower layer.

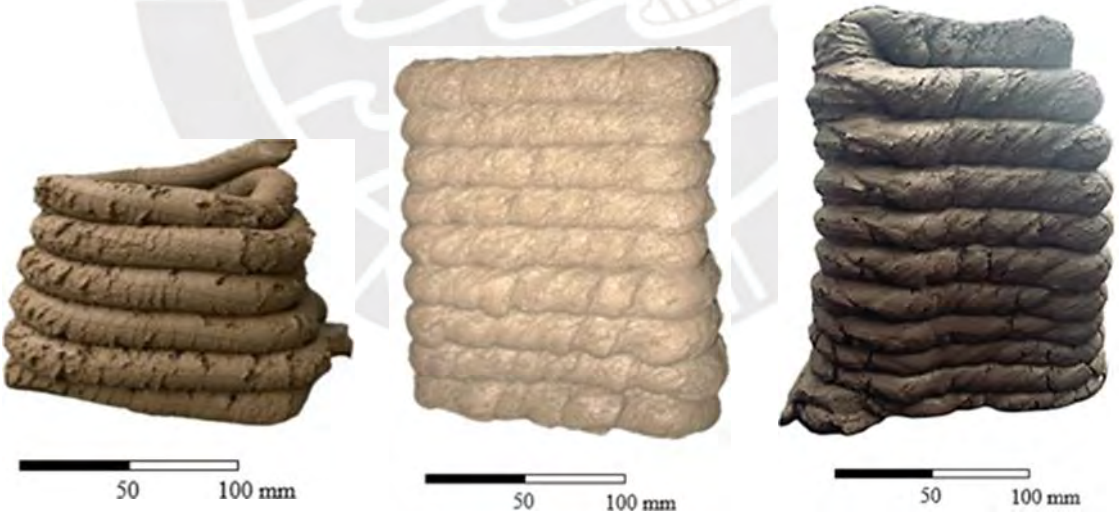

a) SC26 (15%) b) SC27 (15%) c) SC28 (15%)

Figure 4.2. Stacking tests at the concentration of 15% in water contents of a) 26%, b) 27%, and c) 28 %.

4.2. Stage 2: Fresh and hardened state characterization of non-reinforced

4.2.1. Fresh-state characterization

4.2.1.1. Shear stress

The current mechanical test known as the shear vane test was carried out on S22, S23, SC23, SC24, SC25, SC26, SC27, SC28, and SCF samples, non-reinforced and reinforced with jute fibers. S22 and S23 are mixed with only soil and water. Figure 4.4 displayed the changes in shear stress of the matrix prepared with the different water content (%) and fiber reinforcement dosages. The water content is the decisive factor on the shear stress, showing a clear reduction of the value. However, fiber addition as reinforcement showed no remarkable effect. Le et al. (2012) evaluated the mix designs and fresh properties for high-performance concrete resolving that the range from 0.3 to 0.9 kPa is the most suitable for optimum printability as shown in Figure 4.3. Nevertheless, at the moment of printing S22 and S23 filaments, good quality was observed, and a suitable extrusion velocity from both solutions. Hence, the S22 and S23 shear strengths set the standard and an adequate result so the appropriate range was considered 0.3 - 2 kPa of shear stress in the mix dosage.

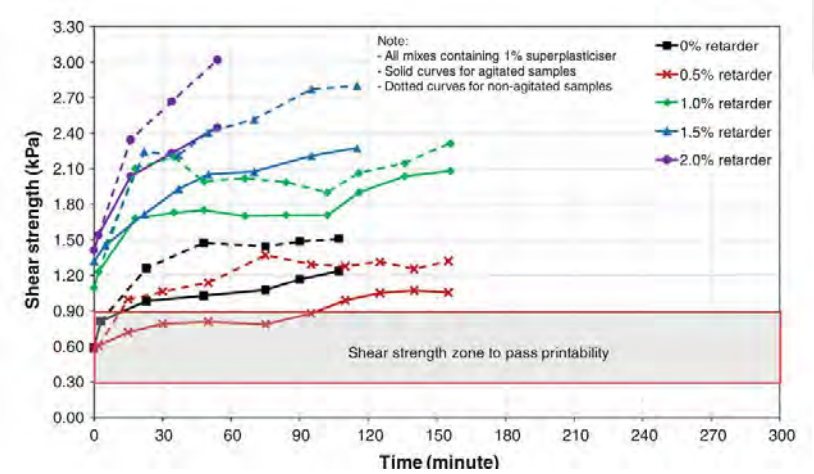

Figure 4.3. Impact of retarder dosage on workability over time (Le et al., 2012).

This information is essential for designing structures and determining appropriate construction techniques. Furthermore, comparing the shear stress values with those of a validated sample, S22 allows a better understanding of the material's performance. As illustrated in Figure 4.4, the satisfactory stability exhibited by SC27, SC28, SCF27, and

SCF278, with the highest OPC content (15%), further supports its suitability for the intended application. However, due to the stacking results in the previous sections, the dosages SC27 and SCF27 will only be considered for further analysis.

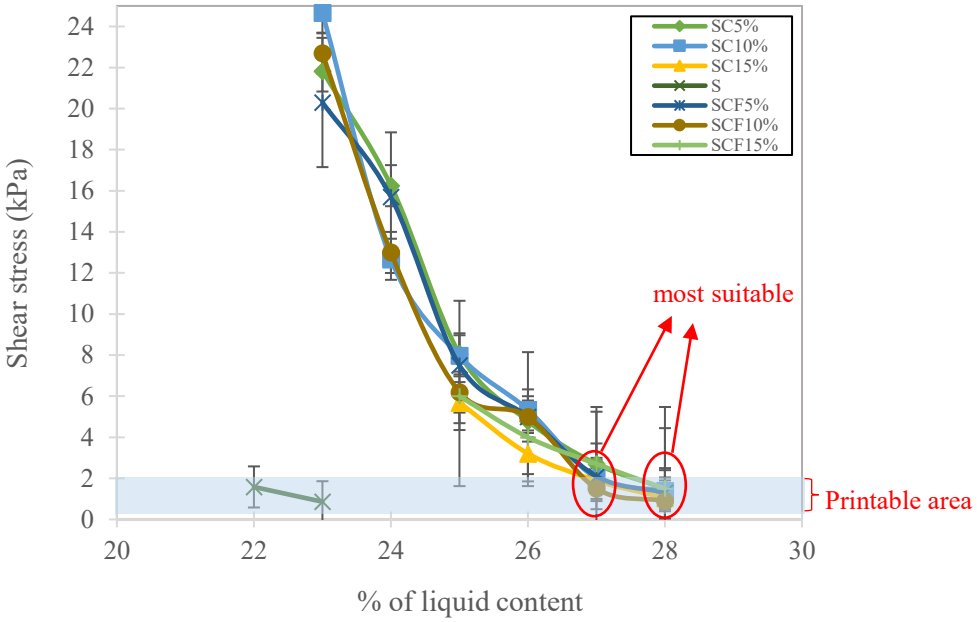

Figure 4.4. Comparison between shear stress with and without jute fibers.

4.2.1.2. Over time shear stress

Over time shear stress was studied to evaluate the stacking quality of the matrix, since impacts directly printability. The maximum shear stress reached is 8 kPa in all matrix samples as seen in Figure 4.5. The non-reinforced matrix SC27 presented similar behaviors regardless of the volume of OPC content. The fiber-reinforced matrix SCF27 (10%) showed no change of shear stress in 10 minutes as a non-reinforced matrix but a linear increase of shear stress with time was observed after 10 minutes.

In the presence of plant fiber reinforcement, the matrix with higher OPC (SCF (15%)) content resulted in faster drying and shear stress increase. SCF27 (15%), reinforced with fibers and containing the highest amount of OPC, showed a remarkable growth of shear stress in a short period by reaching a maximum of 8 kPa in 20 minutes. The results were predictable since the plant fibers are hydrophilic and favor absorbing water (Célino et al., 2014), and the drying speed of cement is faster than the soil. Is worth mentioning that SCF27 (15%) is the

least favorable since it dries faster and the longer it takes to dry the better, since it allows more time to print and the nozzle does not get stuck with the dried matrix.

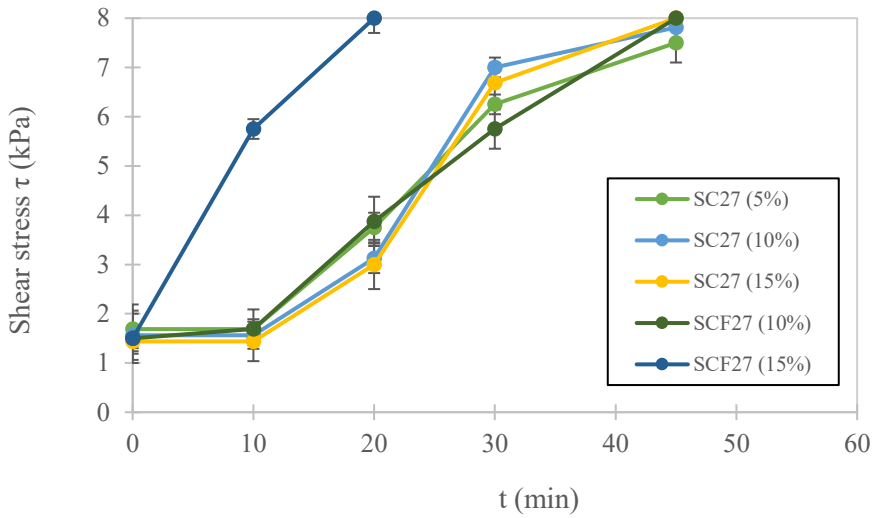

Figure 4.5. Over time in shear stress curves.

4.2.1.3. Vicat test

In Figure 4.6, the results of the Vicat test are presented as the penetration depth with time. The penetration depth represents the initial strength of the matrix and thus the dry condition must play a decisive role. OPC content and fiber reinforcement are important factors in the drying matrix. SCF27 presented as the faster drying than non-reinforced (SC27). The OPC volume content significantly affected the penetration depth, presenting higher OPC content with more resistance to penetration.

Non-reinforced mix-designs, the one with less OPC content (SC27 (5%)) takes more than 5 h to be entirely impenetrable so it dries slower, while the one with more OPC content (SC27 (15%)) dries entirely within 4.5 hours. It can be seen a trend of fiber-free mix designs that take a little longer to dry since the needle can penetrate for more than five hours in the medium point (SC27 (10%)).

On the other hand, fiber-reinforced mixtures can be speculated to dry faster since the fibers help absorb water more quickly, due to the fact it takes four hours as can be seen in Figure 4.6. Within these reinforced mixtures it can be appreciated that higher OPC contents (SC27 (15%)) are appreciated in a more uniform drying process while in lesser OPC contents (SC27 (5%) and SC27 (10%)) this fluctuates more, for example from hour 1 to 2 the pace is faster than from hour 2 to 3 and this one, consequently, to hour 3 to 4.

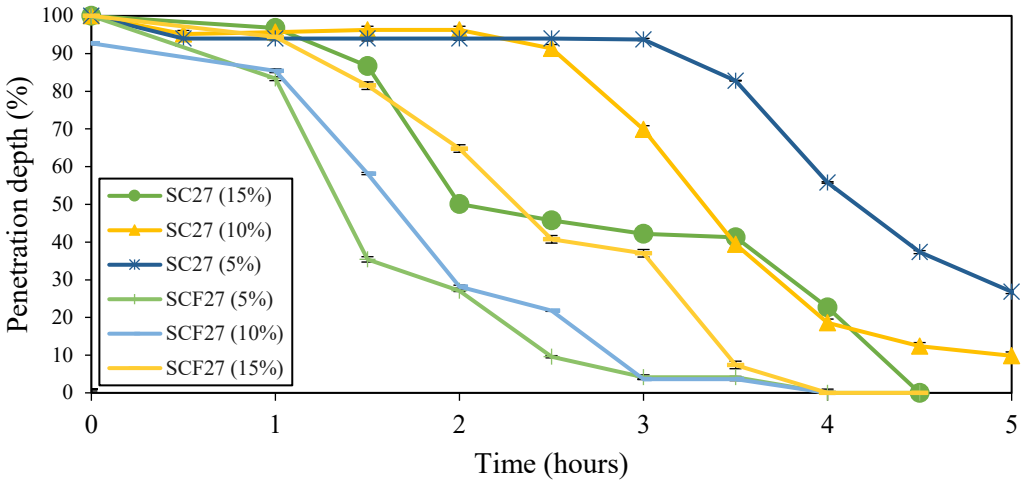

Figure 4.6. Vicat test curves from a mix-design of 27% water with and without jute fibers for 5 hours.

4.2.1.4. Rheological characterization

In the case of rheology, it has been chosen to quantify it through the value of the thixotropy, the yield stress, and the plastic viscosity. For calculating these properties, it was considered the area between the two curves of load and unload of charges for the value of thixotropy, the y-intercept of the unloading curve trending line as the yield stress. The slope of the unloading curve trending line for the plastic viscosity, all three properties shown in Figure 3.5. The mix designs of SC27 (5%), SC27 (10%), and SC27 (15%) graphs are displayed in Figure 4.7, as a, b, and c, respectively.

The thixotropy values increase as the quantity of cement in the solids' weight does; the values are 3220.45, 4552.95, and 8967.23 Pa/s. Regarding the plastic viscosities, they resulted in 4.75, 5.67, and 2.821 Pa.s for the values of OPC of 5, 10, and 15% respectively. Zhang's (2019) findings confirmed that for successful printing in this experiment, the material needed to fall within a viscosity range of 3.8–4.5 Pa.s, a yield stress of 178.5–359.8 Pa, and a thixotropy value below 6284.5 Pa/s. If the thixotropy was too high, the 3D printing concrete materials failed to produce a complete specimen or section, as they either became excessively wet or too rigid to print properly.

As can be perceived in the case of thixotropy, the only one that accomplished this criterion is the SC27 (15%), in the case of viscosity, the closest option near the range was the

SC27 (5%), and all three of them accomplished with the yield stress parameters. Moreover, considering the haptic qualities of the mix designs, it was perceived as a quick dryness and that discouraged the decision to peak at this one as the best mix design. Therefore, the balanced option was the SC27 (10%). Likewise, is worth to mention all the fiber-reinforced specimens were tested as well, however, exceeded the safe limits of the thixotropy of the equipment, demanding to stop the rheometer measuring.

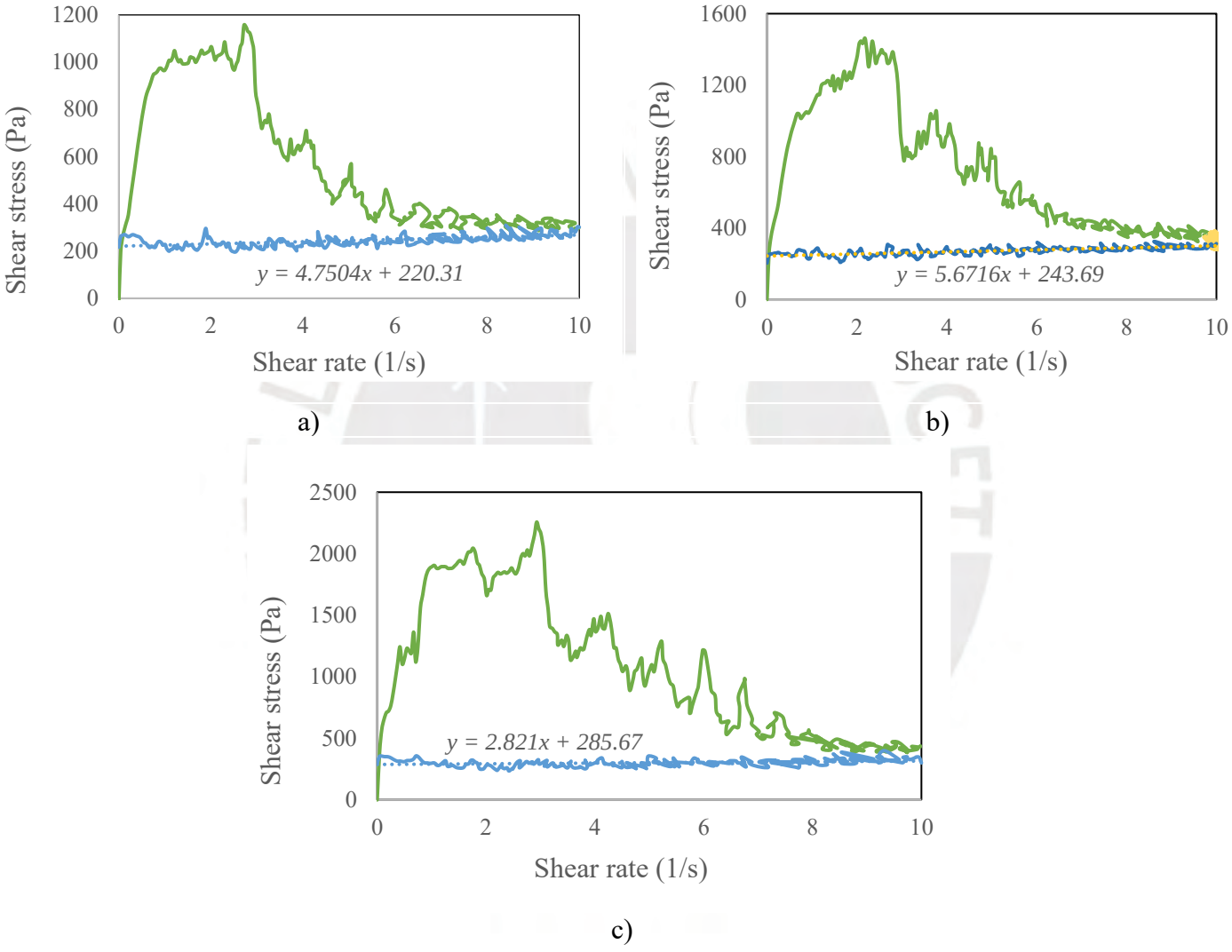

Figure 4.7. Loading and unloading curves of design mixtures a) SC27 (5%), b) SC27 (10%), and c) SC27 (15%)

4.2.2. Hardened-state

4.2.2.1. Elastic modulus

Elastic modulus was studied to verify the mechanical characteristic of the strength of the matrix after curing for 3, 7, and 28 days. The results were presented in Figure 4.8 and proved that the OPC content in the matrix plays a key role in mechanical strength. A dramatic increase was observed when the OPC content increased from 10 to 15 % on both non-reinforced and reinforced matrices with curing time. Similar results were obtained by Nguyen (2024) and discovered by Balmer (1958), which shows that the elastic modulus of soil matrix expanded with the amount of OPC content. The fiber reinforcement slightly influenced the drying state as shown at 28 days between SC27 (15%) and SCF27 (15%) in Figure 4.8. However, no effect on mechanical behavior resulted, presenting no notable differences among the other mixed concentrations.

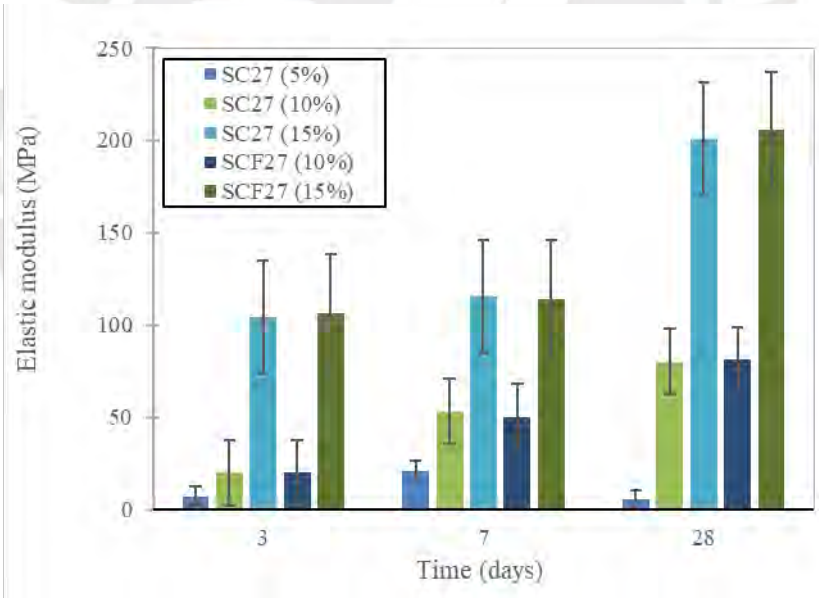

Figure 4.8. Elastic modulus from mix-designs of 27% of water content.

4.2.2.2. Compression test

An increase in compression stress was observed on the matrix with a higher content of OPC as shown in Figure 4.9. However, the value increased with curing time when the matrix with low OPC content (SC27 (5%)) presented a reduction of compression stress and reached its lowest value on the 28th day of curing. Likewise, between 7 days and 28 days, there is a decrease in the compression strength of the SC27 (15%) mix design. On the other hand, SCF27

(10%) has an augmenting pattern not as high as SCF27 (15%). However, an increase overall can be appreciated with most mixed designs.

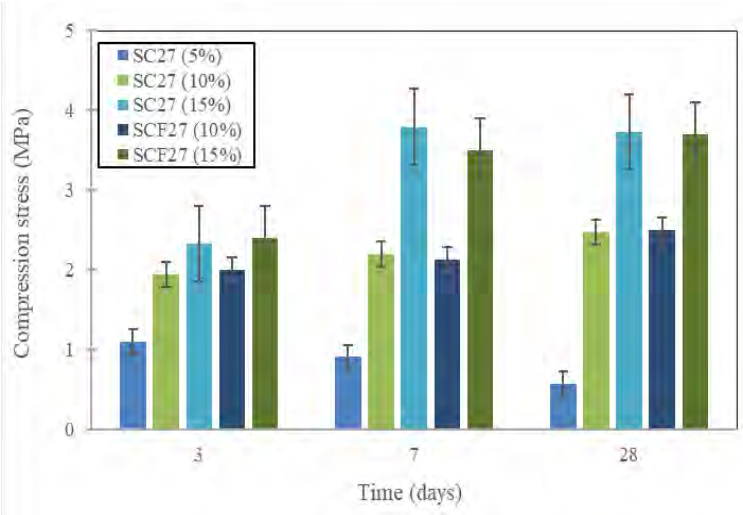

Figure 4.9. Compression stress behavior in 3, 7, and 28 days after printing.

4.2.2.3. Contact-angle test

The findings of the contact-angle tests performed with the cement-stabilized printable soil mixtures SC27 (5%) and SC27 (10%) are shown in Figure 4.10. These were prepared by compressing them into three layers using a tamper and filling them with the mixture in a mold. This methodology allows for obtaining consistent and reproducible samples for subsequent evaluation. Concerning the results obtained, it was determined that the surfaces of the manufactured samples had mainly hydrophobic characteristics, that is, they showed a tendency to repel water. However, some surfaces with hydrophilic traits were also observed, which showed an affinity for water. It is worth mentioning that there were 3D printed samples done with the 3 dosages (SC27 (5, 10, and 15%)), all of them showed hydrophilic behavior with immediate absorption of the water and were not included due to their biased results that could be affected by their pores. Likewise, a hydrophobic behavior can be considered advantageous, hence its perks range from anti-corrosion coverings to anti-icing technologies (Lohatepanont et al., 2024).

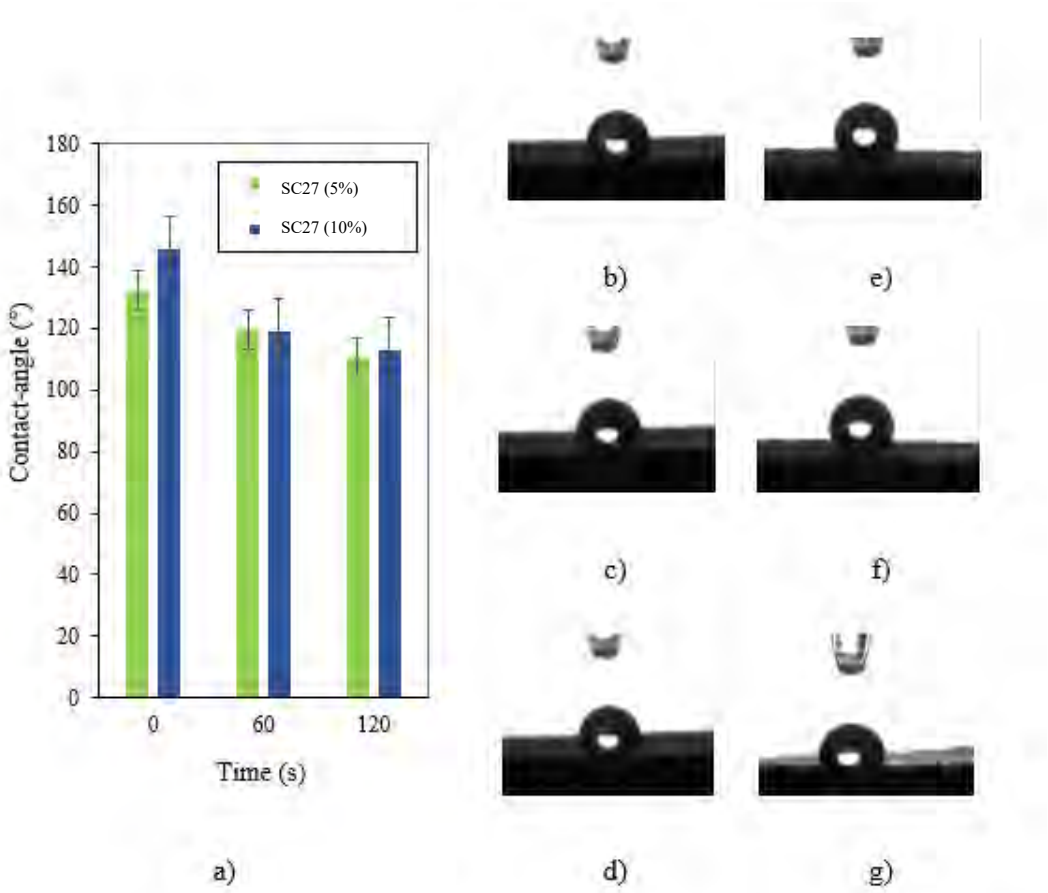

Figure 4.10. Results of the water contact angle test: (a) Contact angles over time for the printable soil mixtures; SC27 (5%) at (b) 0 s; (c) 60 s; (d) 120 s and SC27 (10%) at (e) 0 s; (f) 60 s; and (g) 120 s.

4.2.3. Durability

4.2.3.1. Immersion test

As presented in Figure 4.11, the SC27 sample (5%) showed a total weight loss of 1.9%, while the SC27 sample (10%) recorded a total weight loss of 1.6%. These results indicate that both samples maintained their structural integrity and suffered minimal weight loss during the 28-day curing study period. Also, it could be assured that higher OPC content leads to less erosion and, subsequently, material loss after water immersion.

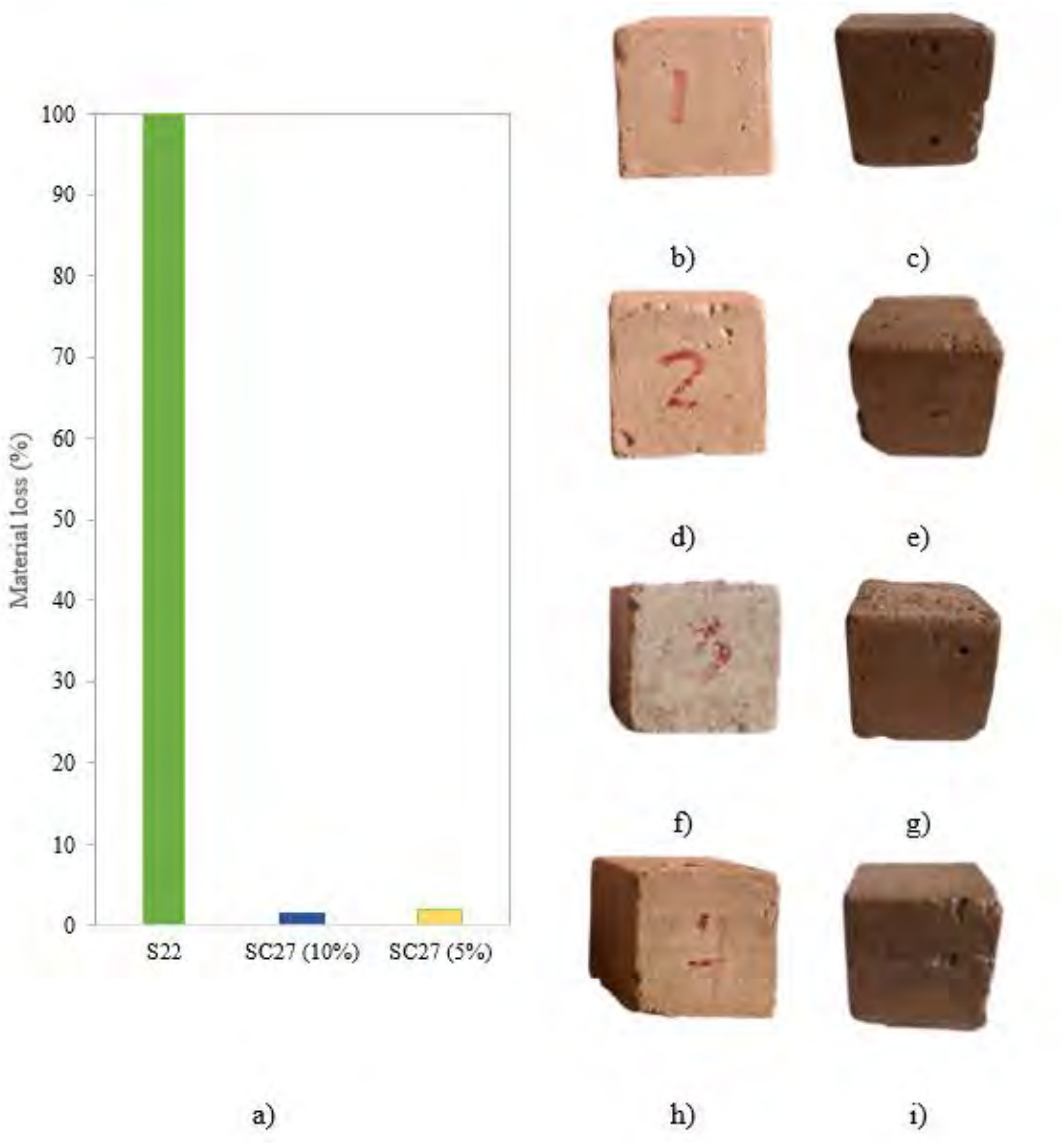

Figure 4.11. Immersion tests: (a) Material loss due to water immersion; samples 1 of SC27 (5%) (b) before; and (c) after; samples 2 of SC27 (5%) (d) before; and (e) after; samples 1 of SC27 (10%) (f) before; and (g) after and samples 2 of SC27 (10%) (h) before; and (i) after.

In addition, the absorption capacity of both mixtures was evaluated. The total

absorption values ranged from 24% to 26%, indicating that the SC27 (5%) and SC27 (10%) mixtures have almost identical absorption capacities. The detailed results and the corresponding graphs are presented in Figure 4.12, where the relationship between weight loss and the absorption capacity of the evaluated mixtures is appreciated.

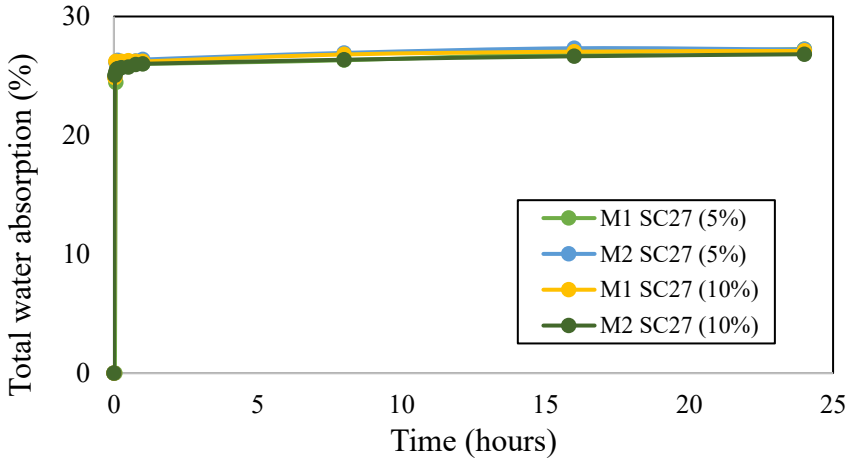

Figure 4.12. Immersion test considering total water absorption.

Therefore, the results indicate that the soil-cement sample at 10% of this on solids, and the mixtures with chitosan presented an insignificant weight loss and had an absorption capacity within the expected range. These findings support the feasibility and potential of the evaluated mixtures for possible application in the corresponding field of study.

4.2.3.2. Accelerated erosion test

During the execution of the test, samples with a minimum height of 200 mm were required. Among the specimens evaluated, specimen SC27 (10%) stood out for its successful performance, showing only surface wetting without crumbling compared to specimen SC22. Detailed results on the accelerated erosion resistance of S22 and SC27 mixtures (10%) are found in Table 5.

After the assay, specimen SC27 (10%) demonstrated remarkable strength and durability, with no evidence of significant deterioration. A slight abrasion was observed in the area in contact with water, indicating its ability to withstand adverse weather conditions, such as high precipitation. Likewise, this statement is supported by the Erodibility index chart from Morel et al (2012) in which the sample is categorized as slightly erosive. These results highlight the suitability of cement stabilization, specifically at a 10% concentration, to provide

a reliable and durable option in environments exposed to severe weather conditions such as precipitation.

Table 5. Comparison between the before and after the accelerated erosion statuses of the mix design S22 and SC27 (10%)

Mix design	Erosion index	3D-printed samples before the erosion test	3D-printed samples after the erosion test
S22	Fail		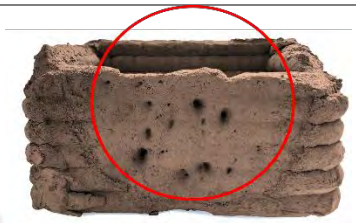
SC27 (10%)	1		

4.3. Stage 3: Medium-scale earthen 3D printing

About medium-scale prints, it was possible to corroborate with the mixture of SC27 (15%) the printability of an 80 cm high sample with a gross area of 37.25 cm x 94.5 cm as displayed in Figure 4.13.b). The Rhinoceros software plus the Grasshopper plugin worked a geometry in the form of adjacent hollow hexagons, as shown in Figure 4.13.c) in plan and isometric in Figure 4.12.a). Settings were the following: print speed of 15 mm/s, 40 mm wide, 20.5 mm high, and 39 layers. There were 11 batches of 25 kg each. The first batch was printed in 25 minutes and the others in approximately 20.

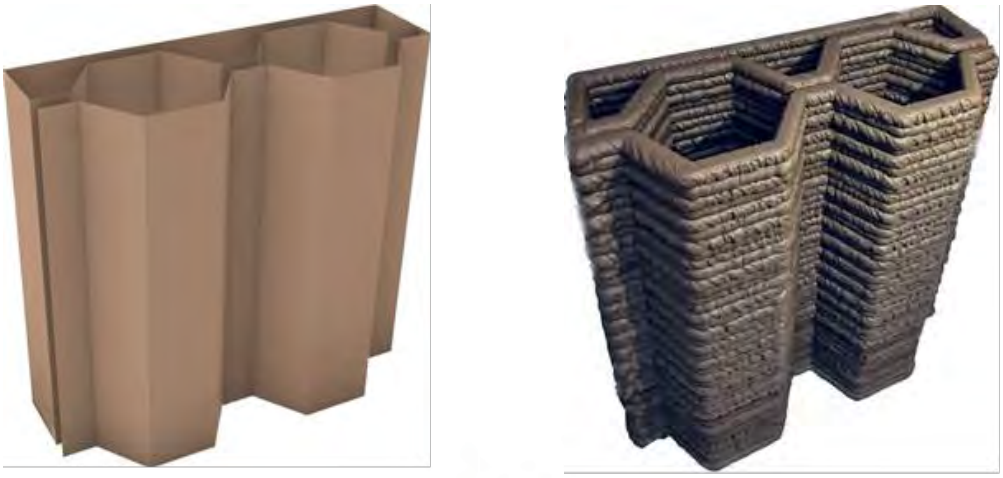

a) b)

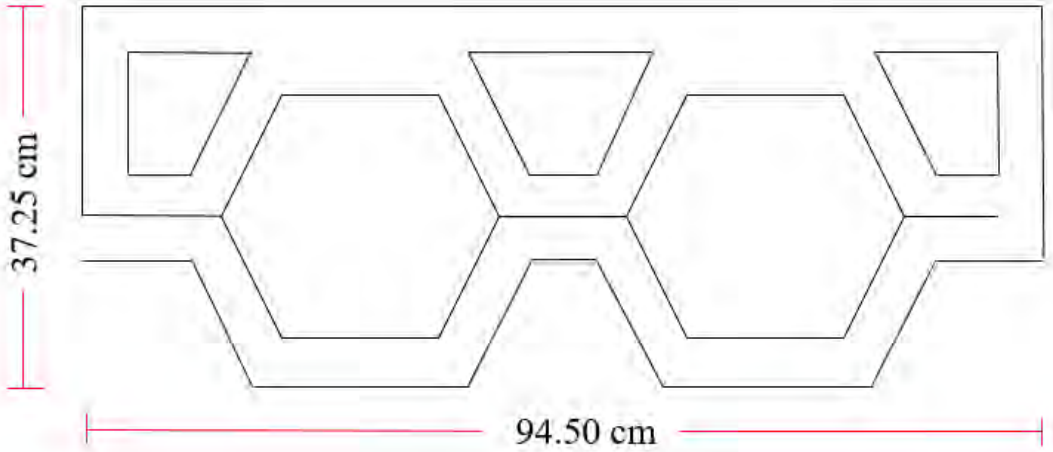

c)

Figure 4.13. Medium-scale 3d printing of soil-cement a) rendered, b) real, and c) its plan view.

4.4. Stage 4: Shrinkage cracking analysis

Cracking is a common issue during the printing process when a wall is constructed with dimensions exceeding the maximum load-bearing capacity of the material. In the case at hand, a wall with dimensions of 80 cm in height and a span of 94.5 cm was printed. Plastic shrinkage problems arose, evidenced by a crack that extended from the outermost layer to 10 layers inward, occurring at the midpoint of the slimmest side, as can be seen in Figure 4.14.

The length of the main and longest fissure was 23 cm, and the width was 2 mm in its thickest section.

a) b)

Figure 4.14. a) Fissure in a soil-cement mix until the eleventh layer downwards, b) Zoom of the fissure.

This type of cracking is frequently observed in 3D-printed concrete mortars due to the formation of negative capillary pressure as pore water evaporates. This pressure leads to volumetric contraction or three-dimensional shrinkage of the material. Cracks could develop when this shrinkage is restricted and the resulting stress exceeds the material's tensile strength (Combrink, 2012). Figure 4.15 illustrates examples of damage caused by shrinkage-induced deformations in 3D-printed concrete. These cracks often extend across multiple layers, compromising the structure’s durability, functionality, and aesthetic quality (Markin et al., 2024).

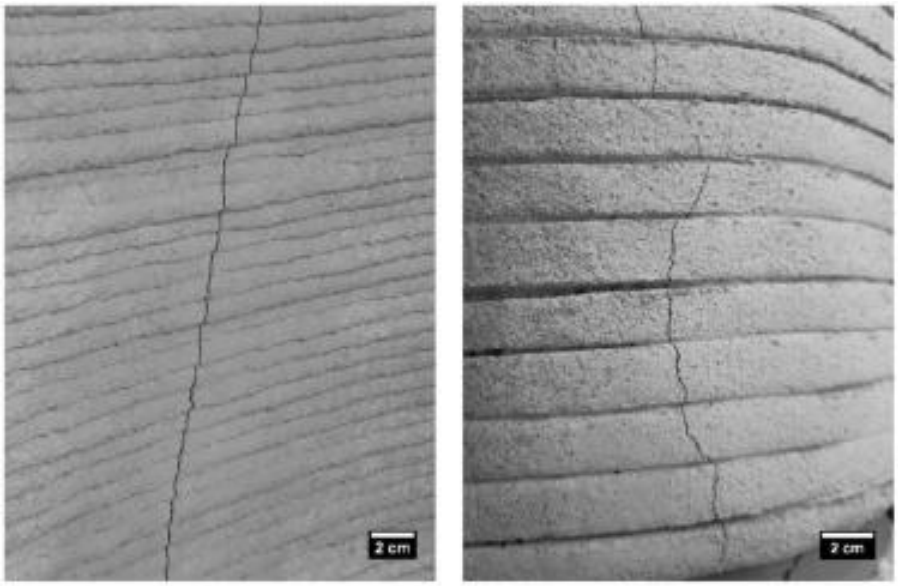

Figure. 4.15. Instances of cracking in 3D-printed concrete structures: (a) the residential building “Project Milestone” in Eindhoven, Netherlands, and (b) the pedestrian and bicycle bridge in Nijmegen, Netherlands (Markin et al., 2024).

Additionally, Table 6 shows a series of samples comprising a stack of 6 printed layers according to Zhang et al (2022). This assay can replicate if cracks occur in a wall due to shrinkage. Different cases of curing conditions were presented to evaluate how their behavior was in each one.

As seen, the curing conditions were 3 according to the conditions exposed to: Sun exposed, non-covered, under the shadow, non-covered, and plastic mantle covered (inside laboratory), and as mentioned above they were small walls of 40 cm long, and 6 filaments stacked. In all the tests, more than 28 days were waited and none of them had a major crack in addition to SC27 (15%) of under shadow, non-covered condition of 2 mm crack width which can occur due to the fast drying due to its high-cement content. Also, the fiber-reinforced mixes did not crack at all.

Table 6. Samples of design mixtures of 27% real water in concentrations of 10% and 15% with and without fibers.

	SC27 (10%)	SCF27 (10%)	SC27 (15%)	SCF27 (15%)
Sun exposed, non-covered				
Under shadow, non-covered				
Plastic mantle covered (inside laboratory)				

4.5. Stage 5: Reinforced medium-scale earthen 3D printing

Samples of SC27 (10%) and SCF27 (10%) were chosen as the best example of best-validated mix-design, the results can be appreciated in Figure 4.16. The one that includes fibers has a percentage of 0.3 from solids weight for fiber content, and both mixes were printed with the same geometry and hexagonal model in plan view. The quality of printing with fibers is much lower than printing without fibers since the 2-inch diameter nozzle is connected to the pump tube that exerts pressure to extrude the material and has a bar that prevents it from being extruded uniformly since in this bar the fiber is congested. The filament quality had many imperfections in the case of fibers due to the congestion of fibers inside the hose.

a) b)

Figure 4.16. Printing of mix-design a) SC27 (10%) and b) SCF27 (10%).

A study of an earthen 3D-printed sample with 15 mm of height per layer shows a crack of approximately 17 cm in length. Markers were placed 130 mm from the center to evaluate the plastic shrinkage and cracking deformation of the 3D-printed mortar under restricted conditions. Images captured during the restrained shrinkage tests were analyzed using a binarization algorithm, with an adjusted threshold to enhance crack visibility. This allowed for the measurement of crack development speed, depth, and width in the 3D-printed mortar samples (Figure 4.16). Concerning the image processing findings, a threshold value of 50 was chosen (Zhang & Xiao, 2021).

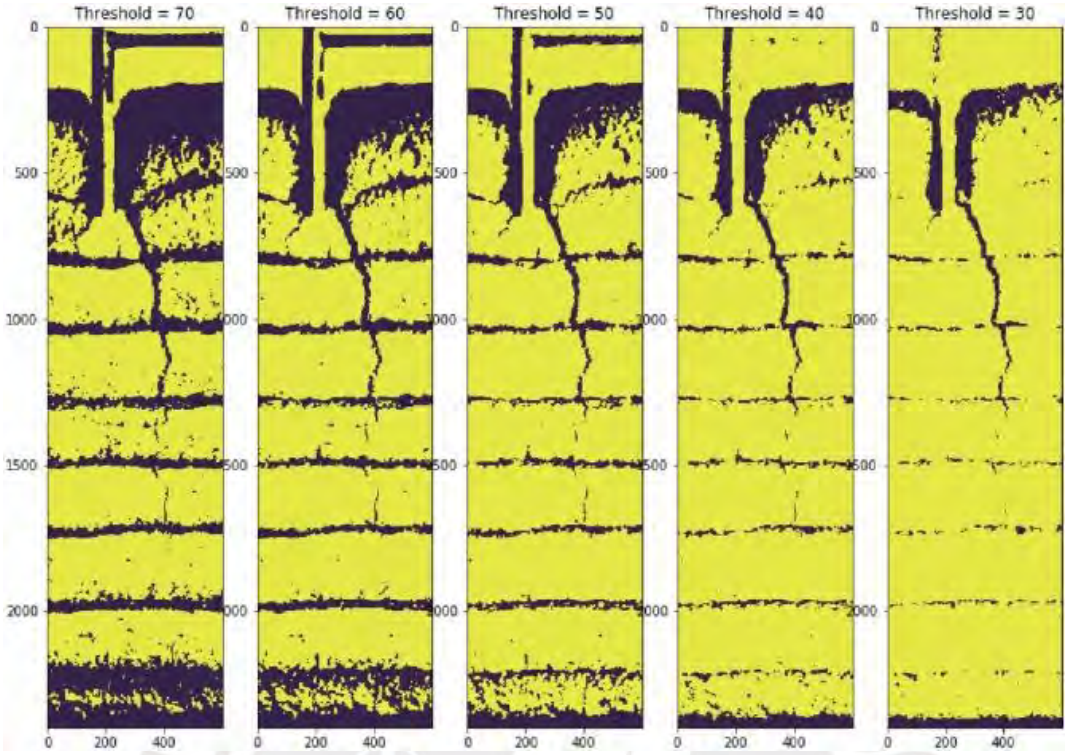

Figure 4.17. Analyzing images of cracks in 3D-printed mortar using various threshold values (Zhang & Xiao, 2021).

Cracks with similar behavior as the Zhang & Xiao study can also be seen in both dosages in Figure 4.18. Having a better result in the short-term (3 days) printing with fibers, as expected in the long term. However. At 28 days, it is seen that the behavior without fiber has been better, having a crack of approximately 2 mm in width and a length of 24.5 cm. Conversely, it was monitored that the specimen that did have fiber was cut along the height of the specimen, which was 64.5 cm, and its width was approximately 3 mm. These results could be affected by several factors, and the main one would be the obstruction of the pump in the dosage with fibers. Hence, it would require other extrusion requirements for these material composites.

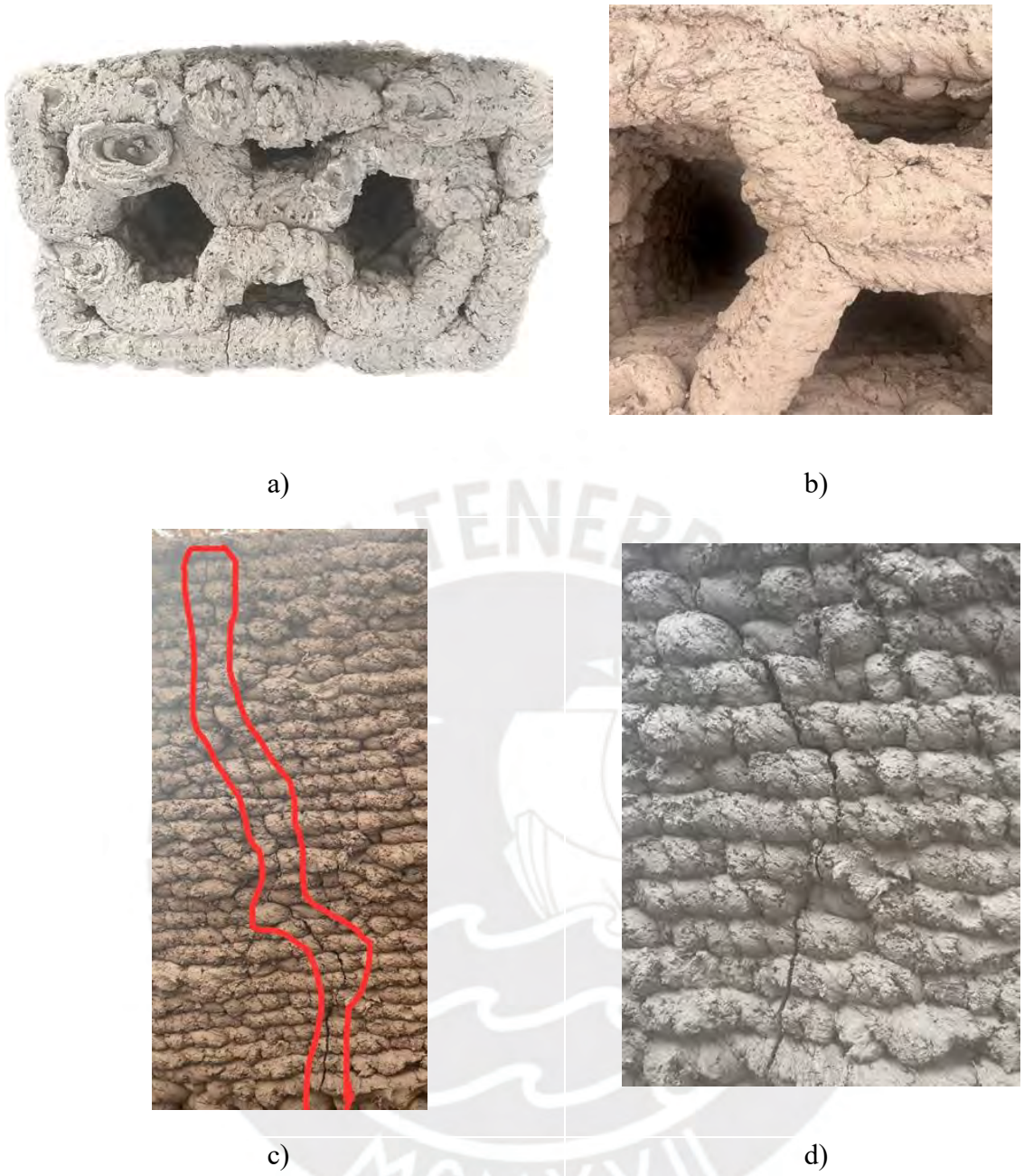

Figure 4.18. Plan view of a) SCF27 (10%), b) SC27 (10%) and Frontal view from c) SCF27 (10%), d) Zoom of SC27 (10%)

Chapter V

Conclusions

This thesis presents a wide-ranging evaluation of the fresh and hardened properties of soil-cement mixtures, with and without jute fiber reinforcement, specifically designed for medium-scale 3D printing applications (ranging from 0.027 to 1 m^3 in printed volume). The findings underscore the substantial improvements in both printability and mechanical performance achieved through the meticulous optimization of mix designs. In particular, the incorporation of Ordinary Portland Cement (OPC) and precise water content control were found to be critical factors in enhancing extrusion quality and the structural stability of printed components. Moreover, jute reinforcement was demonstrated as well to have an impact in the plastic shrinkage analysis.

Mixtures containing 27% water and 10% OPC exhibited superior performance, striking an optimal balance between flowability during extrusion, optimal rheological behavior among all tested formulations, and dimensional stability during stacking. The shear stress analysis demonstrated consistent performance across SC27, SC28, and their fiber-reinforced counterparts. However, the 28% water content formulation was excluded due to excessive deformation and instability during stacking. Additionally, the 15% OPC mixture emerged as a noteworthy alternative, as higher OPC content correlated with enhanced compressive strength and improved hydrophobic properties, resulting in a material less susceptible to corrosion. Nonetheless, the study prioritized minimizing OPC content to enhance sustainability, given that the benefits of increasing OPC beyond 10% did not yield significant performance improvements.

The shrinkage analysis under varying environmental conditions revealed that incorporating 0.3% jute fibers effectively mitigated shrinkage-induced cracking, particularly in small-scale prints, while maintaining material workability. However, fiber inclusion presented extrusion challenges depending on nozzle design, as fiber accumulation could hinder filament deposition and disrupt the printing process.

On the other hand, specimens without fiber reinforcement exhibited visible cracking after seven days, whereas fiber-reinforced samples demonstrated enhanced resistance to shrinkage, maintaining structural integrity for up to twenty-eight days. While these findings are promising, the study was conducted at a laboratory scale using reduced specimen sizes, suggesting that material behavior in large-scale applications may differ. Further research is necessary to validate these findings in real-world construction scenarios.

Finally, the validation tests for medium-scale 3D printing confirm that, with the appropriate equipment and advanced reinforcement methods, it is feasible to utilize the studied materials—water, soil, and cement—for construction applications. A more detailed analysis of crack formation at a larger scale is required to establish a precedent for the study of mix designs within a 3D printing environment for construction. Overall, this examination highlights the potential of earth-cement mixtures reinforced with natural fibers for sustainable 3D printing applications, laying the groundwork for future research and broader implementation in eco-friendly construction practices.

Bibliography

[1] Ali, M. R., Kozan, O., Rahman, A., Islam, K. T., & Hossain, M. I. (2015). Jute retting process: Present practice and problems in Bangladesh. Agricultural Engineering International: CIGR Journal, 17(2).

[2] Alqenaee, A., & Memari, A. (2022). Experimental study of 3D printable cob mixtures. Construction and Building Materials, 324, 126574. https://doi.org/10.1016/j.conbuildmat.2022.126574

[3] Al-Qutaifi, S., Nazari, A., & Bagheri, A. (2018). Mechanical properties of layered geopolymer structures applicable in concrete 3D-printing. Construction and Building Materials, 176, 690-699. https://doi.org/10.1016/j.conbuildmat.2018.04.195

[4] Al-Tamimi, A. K., Alqamish, H. H., Khaldoune, A., Alhaidary, H., & Shirvanimoghaddam, K. (2023). Framework of 3D concrete printing potential and challenges. Buildings, 13(3), 827. https://doi.org/10.3390/buildings13030827.

[5] Alves, L., Leklou, N., & de Barros, S. (2021). Relation between durability and mechanical properties on glass fiber reinforced slag-based geopolymer. Proceedings of the Institution of Mechanical Engineers, Part L: Journal of Materials: Design and Applications, 236(7), 1464-1478. https://doi.org/10.1177/14644207211043870.

[6] Alves, L., Leklou, N., de Souza, F., & De Barros, S. (2021). Assessment of the effect of fiber percentage in glass fiber reinforced slag-based geopolymer. Journal of Asian Ceramic Societies, 9(3), 1265-1274. https://doi.org/10.1080/21870764.2021.1966977.

[7] American Concrete Institute. (2018). CT-18: ACI Concrete Terminology. Farmington Hills, MI: Author. Retrieved from http://www.concrete.org.

[8] Anglade, E., Aubert, J.-E., Sellier, A., & Papon, A. (2022). Physical and mechanical properties of clay–sand mixes to assess the performance of earth construction materials. Journal of Building Engineering, 51, 104229. https://doi.org/10.1016/j.jobe.2022.104229

[9] Anon (2012). Carbon Footprint Assessment Alternative Sites Assessment and Route Selection Report (Phase 2), Dublin: Greater Dublin Drainage.

[10] Anton, A., Reiter, L., Wangler, T., Frangez, V., Flatt, R. J., & Dillenburger, B. (2021). A 3D concrete printing prefabrication platform for bespoke columns. Automation in Construction, 122, 103467. https://doi.org/10.1016/j.autcon.2020.103467.

[11] Apis Cor. (n.d.). We print buildings. http://www.apis-cor.com/

[12] Ashcroft, S. (2024). Top 10: 3D Construction Printing Companies. Construction Digital. Retrieved from https://constructiondigital.com/top10/top-10-3d-construction-printing-companies

[13] Asprone, D., Menna, C., Bos, F. P., Salet, T. A. M., Mata-Falcón, J., & Kaufmann, W. (2018). Rethinking reinforcement for digital fabrication with concrete. Cement and Concrete Research, 112, 111-121. https://doi.org/10.1016/j.cemconres.2018.05.020

[14] Assunção, J., Chadha, K., Vasey, L., Brumaud, C., Zea Escamilla, E., Gramazio, F., Kohler, M., & Habert, G. (2024). Contribution of production processes in environmental impact of low carbon materials made by additive manufacturing. Automation in Construction, 165, 105545. https://doi.org/10.1016/j.autcon.2024.105545

[15] ASTM International (2020). *ASTM C1585-20*: *Standard Test Method for Measurement of Rate of Absorption of Water by Hydraulic-Cement Concretes*. West Conshohocken, PA. https://doi.org/10.1520/C1585-20.

[16] ASTM International. (2021). *ASTM C67-21: Standard test methods for sampling and testing brick and structural clay tile*. ASTM International. https://doi.org/10.1520/C0067-21

[17] ASTM International (2019). *ASTM D2216: Standard Test Methods for Laboratory Determination of Water (Moisture) Content of Soil and Rock by Mass*. West Conshohocken, PA.

[18] ASTM International (2017). *ASTM D4318: Standard Test Methods for Liquid Limit, Plastic Limit, And Plasticity Index of Soils.* West Conshohocken, PA.

[19] ASTM International (2021). *ASTM D6913: Standard Test Methods for Particle-Size Distribution (Gradation) Of Soils Using Sieve Analysis*. West Conshohocken, PA, 2021.

[20] ASTM International (2021). *ASTM D7928: Standard Test Method for Particle-Size Distribution (Gradation) Of Fine-Grained Soils Using the Sedimentation (Hydrometer) Analysis*. West Conshohocken, PA.

[21] ASTM International (2014). *ASTM D854: Standard test methods for specific gravity of soil solids by water pycnometer*. West Conshohocken, PA.

[22] Aubert, J. E., Maillard, P., Morel, J. C., & Al Rafii, M. (2016). Towards a simple compressive strength test for earth bricks? Materials and Structures, 49(5), 1641-1654. https://doi.org/10.1617/s11527-015-0601-y.

[23] Azil, A., Touati, K., Sebaibi, N., Le Guern, M., Streiff, F., Goodhew, S., Gomina, M., & Boutouil, M. (2023). Monitoring of drying kinetics evolution and hygrothermal properties of new earth-based materials using climatic chamber simulation. Case Studies in Construction Materials, 18, e01798. https://doi.org/10.1016/j.cscm.2022.e01798.

[24] Babafemi, A. J., Kolawole, J. T., Chang, Z., & Šavija, B. (2022). Short-term creep and prediction of anisotropic strength of 3D printed concrete under compressive stress. SSRN Electronic Journal. http://dx.doi.org/10.2139/ssrn.4072284.

[25] Bajpayee, A., Farahbakhsh, M., Zakira, U., Pandey, A., Ennab, L. A., Rybkowski, Z., Dixit, M. K., Schwab, P. A., Kalantar, N., & Birgisson, B. (2020). In situ resource utilization and reconfiguration of soils into construction materials for the additive manufacturing of buildings. Frontiers in Materials, 7, 52. https://doi.org/10.3389/fmats.2020.00052.

[26] Balmer, G. G. (1958). *Shear strength and elastic properties of soil-cement mixtures under triaxial loading* (No. D-32).

[27] Bester, F., van den Heever, M., Kruger, J., & van Zijl, G. (2021). Reinforcing digitally fabricated concrete: A systems approach review. Additive Manufacturing, 37, 101737. https://doi.org/10.1016/j.addma.2020.101737.

[28] Boghossian, E., & Wegner, L. D. (2008). Use of flax fibres to reduce plastic shrinkage cracking in concrete. Cement and Concrete Composites, 30(10), 929-937. https://doi.org/10.1016/j.cemconcomp.2008.09.003

[29] Bohuchval, M., Sonebi, M., Amziane, S., Perrot, A., 2020. Effect of metakaolin and natural fibres on three-dimensional printing mortar. Proceedings of the Institution of Civil Engineers – Construction Materials, (2020). https://doi.org/10.1680/jcoma.20.00009.

[30] Bos, F. P., Ahmed, Z. Y., Jutinov, E. R., & Salet, T. A. M. (2017). Experimental exploration of metal cable as reinforcement in 3D printed concrete. Materials, 10(11), 1314. https://doi.org/10.3390/ma10111314.

[31] Bos, F. P., Bosco, E., & Salet, T. A. M. (2019). Ductility of 3D printed concrete reinforced with short straight steel fibers. Virtual and Physical Prototyping, 14(2), 160-174. https://doi.org/10.1080/17452759.2018.1548069.
[32] Broeren, M. L. M., Dellaert, S. N. C., Cok, B., Patel, M. K., Worrell, E., & Shen, L. (2017). Life cycle assessment of sisal fibre – Exploring how local practices can influence environmental performance. Journal of Cleaner Production, 149, 818-827. https://doi.org/10.1016/j.jclepro.2017.02.073.
[33] Carcassi, O. B., Maierdan, Y., Akemah, T., Kawashima, S., & Ben-Alon, L. (2024). Maximizing fiber content in 3D-printed earth materials: Printability, mechanical, thermal and environmental assessments. Construction and Building Materials, 425, 135891. https://doi.org/10.1016/j.conbuildmat.2024.135891.
[34] Castoldi, R., Liebscher, M., de Souza, L.M.S., Mechtcherine, V., Silva, F.A., 2024. Tensile creep behavior of sisal fibers under different environmental conditions, Journal of Material Science. https://doi.org/10.1007/s10853-024-09427-5
[35] Célino, A., Fréour, S., Jacquemin, F., & Casari, P. (2014). The hygroscopic behavior of plant fibers: A review. Frontiers in Chemistry, 1(2013), 43. https://doi.org/10.3389/fchem.2013.00043
[36] Centre for the Development of Industry, & CRATerre-EAG. (1998). Compressed Earth Blocks Standards. Retrieved from https://www.nzdl.org/cgi-bin/library?e=d-00000-00---off-0cdl--00-0----0-10-0---0---0direct-10---4-------0%E2%80%930%E2%80%89l--11-en-50---20-about---00-0-1-00-0-0-11-1-0utfZz-8-10&cl=CL4.30&d=HASH01979938ef89e979ddfb736b&gt=2.
[37] Cesaretti, G., Dini, E., De Kestelier, X., Colla, V., & Pambaguian, L. (2014). Building components for an outpost on the Lunar soil by means of a novel 3D printing technology. Acta Astronautica, 93, 430-450. https://doi.org/10.1016/j.actaastro.2013.07.034.
[38] CGTN. (2018). World's first 3D-printed bus stop installed in Shanghai. The State Council The People's Republic of China. Retrieved from https://english.www.gov.cn/news/video/2018/01/14
[39] Chen, Y., Jansen, K., Zhang, H., Romero Rodriguez, C., Gan, Y., Çopuroğlu, O., & Schlangen, E. (2020). Effect of printing parameters on interlayer bond strength of 3D printed limestone-calcined clay-based cementitious materials: An experimental and numerical study. Construction and Building Materials, 262, 120094. https://doi.org/10.1016/j.conbuildmat.2020.120094.
[40] Choi, M. S., Kim, Y. J., & Kim, J. K. (2014). Prediction of concrete pumping using various rheological models. International Journal of Concrete Structures and Materials, 8(3), 269-278. https://doi.org/10.1007/s40069-014-0084-1.
[41] Combrinck, R., & Boshoff, W. P. (2012). Theory for the early age plastic cracking behaviour of concrete. In fib PhD Symposium (pp. 1-10). Karlsruhe, Germany. https://doi.org/10.1016/j.conbuildmat.2022.128007
[42] Construction Industries Division of the Regulation and Licensing Department. (2023). 2021 New Mexico Earthen Building Materials Code. Retrieved from https://www.srca.nm.gov/parts/title14/14.007.0004.html
[43] Contour3D. (2023, May). Australia's first 3D printed home with full occupation certificate. Contour3D. Retrieved from https://contour3d.com.au/australias-first-3d-printed-home-with-full-occupation-certificate/
[44] CRATerre (2021) CRATerre, CRATerre.
[45] Cui, W., Shen, L., Ji, D., Liu, W., Wang, T., & Hou, D. (2024). Mechanical performance and permeability of low-carbon printable concrete. Journal of Sustainable Cement-Based Materials, 13(2), 237-4839. https://doi.org/10.1080/21650373.2024.2374839.
[46] Curth, A., Pearl, N., Castro-Salazar, A., Mueller, C., & Sass, L. (2024). 3D printing

earth: Local, circular material processing, fabrication methods, and Life Cycle Assessment. Construction and Building Materials, 421, 135714. https://doi.org/10.1016/j.conbuildmat.2024.135714.
[47] CyBe Construction. (2024). Earthquake-proof houses with 3D concrete printing. CyBe Construction. Retrieved from https://cybe.eu/affordable-housing/earthquake-proof-houses/
[48] Dahl, P. (1986). Influence of fibre reinforcement on plastic shrinkage and cracking. In Brittle Matrix Composites. Proceedings of the First European Mechanical Colloquium.
[49] De Andrade Silva F., Chawla N., Toledo Filho R.D. (2008). Tensile behavior of high performance natural (sisal) fibers, Composites Science and Technology, 68, 15–16, pp. 3438-3443. https://doi.org/10.1016/j.compscitech.2008.10.001
[50] Ding, T., Xiao, J., Zou, S., & Zhou, X. (2020). Anisotropic behavior in bending of 3D printed concrete reinforced with fibers. Composite Structures, 254, 112808. https://doi.org/10.1016/j.compstruct.2020.112808
[51] Dobson, S. (2014). Rammed earth in the modern world. Semantic Scholar. Retrieved from https://www.semanticscholar.org/paper/Rammed-earth-in-the-modern-world-Dobson/8f9f5754a3e7e3ae474e61b3a16024113919adbc
[52] Duboust, O. (2023). This company has 3D-printed a house that can withstand a 9.0 magnitude earthquake. Euronews. Retrieved from https://www.euronews.com/next/2023/10/25/this-company-has-3d-printed-a-house-that-can-withstand-a-90-magnitude-earthquake
[53] EN 197–1. (2011). Cement Composition, specifications and conformity criteria for common cements, CEN, Comité européen de normalization, Brussels, Belgium, p. 52.
[54] Fabbri, A., Morel, J. C., Aubert, J. E., Bui, Q. B., Gallipoli, D., & Venkatarama Reddy, B. (2022). Testing and characterisation of earth-based building materials and elements: State-of-the-art report of the RILEM TC 274-TCE. Springer Cham. https://doi.org/10.1007/978-3-030
[55] Faleschini, F., Trento, D., Masoomi, M., Pellegrino, C., & Zanini, M. A. (2023). Sustainable mixes for 3D printing of earth-based constructions. Construction and Building Materials, 398, 132496. https://doi.org/10.1016/j.conbuildmat.2023.132496
[56] Fidelis, M.E.A., Pereira, T.V.C., Martins Gomes, O. F., de Andrade Silva, F., Toledo Filho R. D. (2013). The effect of fiber morphology on the tensile strength of natural fibers, Journal of Materials Research and Technology, 2, 2, 149-157. https://doi.org/10.1016/j.jmrt.2013.02.003.
[57] Figueiredo, S. C., Rodríguez, C. R., Ahmed, Z. Y., Bos, D. H., Xu, Y., Salet, T. M., Çopuroğlu, O., Schlangen, E., & Bos, F. P. (2019). An approach to develop printable strain hardening cementitious composites. Materials & Design, 169, 107651. https://doi.org/10.1016/j.matdes.2019.107651.
[58] Figueiredo, S. C., Rodríguez, C. R., Ahmed, Z. Y., Bos, D. H., Xu, Y., Salet, T. M., Çopuroğlu, O., Schlangen, E., & Bos, F. P. (2020). Mechanical behavior of printed strain hardening cementitious composites. Materials, 13(10), 2253. https://doi.org/10.3390/ma13102253.
[59] Food and Agriculture Organization of the United Nations. (n.d.). Future fibres home. FAO. Retrieved December 14, 2024, from https://www.fao.org/economic/futurefibres/home/en/
[60] Food and Agriculture Organization of the United Nations. (n.d.). Harmonized World Soil Database (Version 1.2). FAO SOILS PORTAL. Retrieved December 14, 2024, from https://www.fao.org/soils-portal/data-hub/soil-maps-and-databases/harmonized-world-soil-database-v12/en/.
[61] Fritz Benachio, G. L., Freitas, M. d. C. D., & Tavares, S. F. (2020). Circular economy in the construction industry: A systematic literature review. Journal of Cleaner Production,

260, 121046. https://doi.org/10.1016/j.jclepro.2020.121046
[62] Furet, B., Poullain, P., & Garnier, S. (2019). 3D printing for construction based on a complex wall of polymer-foam and concrete. Additive Manufacturing, 28, 58-64. https://doi.org/10.1016/j.addma.2019.04.002.
[63] Geng, Z., She, W., Zuo, W., Lyu, K., Pan, H., Zhang, Y., & Miao, C. (2020). Layer-interface properties in 3D printed concrete: Dual hierarchical structure and micromechanical characterization. Cement and Concrete Research, 138, 106220. https://doi.org/10.1016/j.cemconres.2020.106220.
[64] Global Market Insights. (2024). *3D Printing in Construction Market Size, Global Trends 2024-2032*. Recuperado de https://www.gminsights.com/industry-analysis/3d-printing-in-construction-market.
[65] Gomaa, M., Jabi, W., Soebarto, V., & Xie, Y. M. (2022). Digital manufacturing for earth construction: A critical review. Journal of Cleaner Production, 338, 130630. https://doi.org/10.1016/j.jclepro.2022.130630.
[66] Gomaa, M., Jabi, W., Veliz Reyes, A., & Soebarto, V. (2021). 3D printing system for earth-based construction: Case study of cob. Automation in Construction. https://doi.org/10.1016/j.autcon.2021.103577
[67] Gosselin, C., Duballet, R., Roux, P., Gaudillière, N., Dirrenberger, J., & Morel, P. (2016). Medium-scale 3D printing of ultra-high performance concrete – a new processing route for architects and builders. Materials & Design, 100, 102-109. https://doi.org/10.1016/j.matdes.2016.03.097.
[68] Grasselly, D., Hamm, F., Quaranta, G., & Vitrou, J. (2009). Carbon footprint of coconut fibre (coir) substrates. Infos-Ctifl, 2009(249), 55-59. https://doi.org/10.5555/20093081674.
[69] Hack, N., Dörfler, K., Walzer, A. N., Wangler, T., Mata-Falcón, J., Kumar, N., Buchli, J., Kaufmann, W., Flatt, R. J., Gramazio, F., & Kohler, M. (2020). Structural stay-in-place formwork for robotic in situ fabrication of non-standard concrete structures: A real scale architectural demonstrator. Automation in Construction, 115, 103197. https://doi.org/10.1016/j.autcon.2020.103197.
[70] Hamard, E., Cazacliu, B., Razakamanantsoa, A., & Morel, J. C. (2016). Cob, a vernacular earth construction process in the context of modern sustainable building. Building and Environment, 106(1), 103-119. https://doi.org/10.1016/j.buildenv.2016.06.009
[71] Hammond, G., & Jones, C. (2008). Inventory of Carbon & Energy (ICE) Version 1.6a. University of Bath. Retrieved from https://www.appropedia.org/w/images/5/56/ICE_Version_1.6a.pdf.
[72] Han, N., Xiao, J., Zhang, L., & Peng, Y. (2022). A microscale-based numerical model for investigating hygro-thermo-mechanical behaviour of 3D printed concrete at elevated temperatures. Construction and Building Materials, 344, 128231. https://doi.org/10.1016/j.conbuildmat.2022.128231.
[73] Han, Y., Yang, Z., Ding, T., & Xiao, J. (2021). Environmental and economic assessment on 3D printed buildings with recycled concrete. Journal of Cleaner Production, 278, 123884. https://doi.org/10.1016/j.jclepro.2020.123884.
[74] Harrison, R. (1999). Earth: The conservation and repair of Bowhill, Exeter: Working with cob. Engineering, Environmental Science, History. Retrieved from https://www.semanticscholar.org/paper/Earth-%3A-the-conservation-and-repair-of-Bowhill%2C-%3A-Harrison/8cd20ae9af774ce643d9a2703d41e3fc38db7858
[75] Hassan, H., Rodriguez-Ubinas, E., Al Tamimi, A., Trepci, E., Mansouri, A., & Almehairbi, K. (2024). Towards innovative and sustainable buildings: A comprehensive review of 3D printing in construction. Automation in Construction, 163, 105417.

https://doi.org/10.1016/j.autcon.2024.105417
[76] Heathcote, K. A. (1995). Durability of earthwall buildings. Construction and Building Materials, 9(3), 185-189. https://doi.org/10.1016/0950-0618(95)00035-E
[77] Hebel, D. E., & Heisel, F. (2017). Cultivated Building Materials: Industrialized Natural Resources for. Birkhäuser. https://books.google.com/books?hl=es&lr=&id=iItsDwAAQBAJ&oi=fnd&pg=PA5&ots=7xpjk5JrJP&sig=kixCEhNed-XE1d22jzQVXKUs1nU#v=onepage&q&f=false
[78] Hejazi, S. M., Sheikhzadeh, M., Abtahi, S. M., & Zadhoush, A. (2012). A simple review of soil reinforcement by using natural and synthetic fibers. Construction and Building Materials, 30, 100-116. https://doi.org/10.1016/j.conbuildmat.2011.11.045
[79] Huyen, B. T., Hussain, M., & Levacher, D. (2022). Recycling of tropical natural fibers in building materials. In Natural Fiber [Working Title]. IntechOpen. https://doi.org/10.5772/intechopen.102999
[80] ICON. (2022). House Zero. Retrieved from https://www.iconbuild.com/projects/house-zero.
[81] ICON. (2021). Mars Dune Alpha. Retrieved from https://www.iconbuild.com/projects/mars-dune-alpha.
[82] ICON Team. (2022). The Genesis Collection at Wolf Ranch. ICON. Retrieved from https://www.iconbuild.com/projects/the-genesis-collection-at-wolf-ranch
[83] IndustryARC. (2022). 3D Concrete Printing Market Share, Size and Industry Growth Analysis 2022-2027. Retrieved from https://www.industryarc.com/Research/3D-Concrete-Printing-Market-Research-503180
[84] Iribar, I. (2023). How 3D printing in the construction industry works. Cemex Ventures. Retrieved from https://www.cemexventures.com/3d-printing-in-construction/
[85] ISO. (2024). International Organization for Standardization. Retrieved from https://www.iso.org/home.html
[86] ISO/ASTM International (2016). ISO/ASTM 52915:2016 - Additive manufacturing — Specification for additive manufacturing file format (AMF) — Version 1.2. International Organization for Standardization and ASTM International. Retrieved from https://www.iso.org/standard/67472.html
[87] ISO/ASTM International (2017). ISO/ASTM 52901:2017 - Additive manufacturing — General principles — Requirements for purchased AM parts. International Organization for Standardization and ASTM International. Retrieved from https://www.iso.org/standard/67288.html#:~:text=ISO%2FASTM%2052901%3A2017%20gives%20guidelines%20for%20the%20elements%20to,final%20part%20characteristics%20and%20properties%2C%20inspection%20requirements%20and
[88] ISO/ASTM International (2018). ISO/ASTM 52910:2018 - Additive manufacturing — Design — Requirements, guidelines, and recommendations. International Organization for Standardization and ASTM International. Retrieved from https://www.iso.org/obp/ui/#iso:std:iso-astm:52910:ed-1:v1:en
[89] ISO/ASTM International (2021). ISO/ASTM 52900:2021 - Additive manufacturing — General principles — Fundamentals and vocabulary. International Organization for Standardization and ASTM International. Retrieved from https://www.iso.org/standard/74514.html
[90] ISO/ASTM International (2023). ISO/ASTM 52939:2023 - Additive manufacturing for construction — Qualification principles — Structural and infrastructure elements. International Organization for Standardization and ASTM International. Retrieved from https://www.iso.org/standard/81177.html
[91] Ji, G., Ding, T., Xiao, J., Du, S., Li, J., & Duan, Z. (2019). A 3D printed ready-mixed concrete power distribution substation: Materials and construction technology. Materials,

12(9), 1540. https://doi.org/10.3390/ma12091540.
[92] Ji, Y., Poullain, P., & Leklou, N. (2023). The selection and design of earthen materials for 3D printing. Construction and Building Materials, 404, 133114. https://doi.org/10.1016/j.conbuildmat.2023.133114
[93] JK Cement. (2024). Understanding the utility of 3D printing in construction. JK Cement. Retrieved from https://www.jkcement.com/blog/construction-planning/3d-printing-in-construction/
[94] Khan, M. A., Rahaman, M. S., Al-Jubayer, A., & Islam, J. M. M. (2015). Modification of jute fibers by radiation-induced graft copolymerization and their applications. In V. K. Thakur (Ed.), Cellulose-Based Graft Copolymers: Structure and Chemistry (pp. 209-234). CRC Press. https://doi.org/10.1201/b18390-12
[95] Khan, M. S., Sanchez, F., & Zhou, H. (2020). 3-D printing of concrete: Beyond horizons. Cement and Concrete Research, 133, 106070. https://doi.org/10.1016/j.cemconres.2020.106070.
[96] Khoshnevis, B., Hwang, D., Yao, K.-T., & Yeh, Z. (2006). Mega-scale fabrication by Contour Crafting. International Journal of Industrial and Systems Engineering, 1(3), 301-320. https://doi.org/10.1504/IJISE.2006.009791.
[97] Kloft, H., Oechsler, J., Loccarini, F., Gosslar, J., & Delille, C. (2019). Robotische Fabrikation von Bauteilen aus Stampflehm. DBZ Deutsche BauZeitschrift, 7-8. https://doi.org/10.17104/9783406736605.
[98] Kremenetsky, M. (2022). The largest 3D-printed affordable housing project built. Holcim. Retrieved from https://3dprint.com/291593/3d-printed-school-and-tiny-house-set-additive-construction-precedents-for-cobod/
[99] Kruger, J., Zeranka, S., & van Zijl, G. (2019). 3D concrete printing: A lower bound analytical model for buildability performance quantification. Automation in Construction, 106, 102904. https://doi.org/10.1016/j.autcon.2019.102904.
[100] Ler, K.-H., Ma, C.-K., Chin, C.-L., Ibrahim, I. S., Padil, K. H., & Ab Ghafar, M. A. I. (2024). Porosity and durability tests on 3D printing concrete: A review. Construction and Building Materials, 446, 137973. https://doi.org/10.1016/j.conbuildmat.2024.137973.
[101] Le, T. T., Austin, S. A., Lim, S., Buswell, R. A., Gibb, A. G. F., & Thorpe, T. (2012). Mix design and fresh properties for high-performance printing concrete. Materials and Structures, 45(8), 1221-1232. https://doi.org/10.1617/s11527-012-9828-z
[102] Li, H., Addai-Nimoh, A., Kreiger, E., Khayat, K. H. (2024). Methodology to design eco-friendly fiber-reinforced concrete for 3D printing, Cement and Concrete Composites, 147, 105415. https://doi.org/10.1016/j.cemconcomp.2023.105415.
[103] Lim, S., Buswell, R., Le, T., Wackrow, R., Austin, S., Gibb, A., & Thorpe, T. (2011). Development of a viable concrete printing process. In Proceedings of the 28th International Symposium on Automation and Robotics in Construction (ISARC) (pp. 665-670). https://doi.org/10.22260/ISARC2011/0124.
[104] Li, Z., Wang, L., Ma, G., Sanjayan, J., & Feng, D. (2020). Strength and ductility enhancement of 3D printing structure reinforced by embedding continuous micro-cables. Construction and Building Materials, 264, 120196. https://doi.org/10.1016/j.conbuildmat.2020.120196.
[105] Lohatepanont, M., Chen, M., Mendoza Nova, L. C., Murray, J.-T., & Merchan-Merchan, W. (2024). Exploring microstructure patterns: Influence on hydrophobic properties of 3D-printed surfaces. Micro, 4(3), 442-459. https://doi.org/10.3390/micro4030028
[106] Lura, P., Toropovs, N., Justs, J., Shakoorioskooie, M., Münch, B., & Griffa, M. (2024). Mitigation of plastic shrinkage cracking with natural fibers - kenaf, abaca, coir, jute and sisal. Cement and Concrete Composites, 155, 105827.

https://doi.org/10.1016/j.cemconcomp.2024.105827.
[107] Majumder, A., Stochino, F., Farina, I., Valdes, M., Fraternali, F., & Martinelli, E. (2022). Physical and mechanical characteristics of raw jute fibers, threads and diatons. Construction and Building Materials, 326, 126903. https://doi.org/10.1016/j.conbuildmat.2022.126903
[108] Ma, L., Zhang, Q., Jia, Z., Liu, C., Deng, Z., & Zhang, Y. (2022). Effect of drying environment on mechanical properties, internal RH and pore structure of 3D printed concrete. Construction and Building Materials, 315, 125731. https://doi.org/10.1016/j.conbuildmat.2021.125731.
[109] Malaeb, Z., Hachem, H., Tourbah, A., Maalouf, T., El Zarwi, N., & Hamzeh, F. (2015). 3D concrete printing: Machine and mix design. International Journal of Civil Engineering and Technology, 6(6), 14-22. https://www.researchgate.net/publication/280488795_3D_Concrete_Printing_Machine_and_Mix_Design.
[110] Marchment, T., & Sanjayan, J. (2020). Mesh reinforcing method for 3D Concrete Printing. Automation in Construction, 109, 102992. https://doi.org/10.1016/j.autcon.2019.102992.
[111] Mario Cucinella Architects. (2024). TECLA – Technology and Clay. Mario Cucinella Architects. Retrieved from https://www.mcarchitects.it/en/projects/tecla-technology-and-clay.
[112] McKinsey Global Institute (2017). Reinventing Construction: A Route to Higher Productivity, pp1-9
[113] McLellan, B. C., Williams, R. P., Lay, J., van Riessen, A., & Corder, G. D. (2011). Costs and carbon emissions for geopolymer pastes in comparison to ordinary portland cement. Journal of Cleaner Production, 19(9-10), 1080-1090. https://doi.org/10.1016/j.jclepro.2011.02.010.
[114] Mechtcherine, V., Grafe, J., Nerella, V. N., Spaniol, E., Hertel, M., & Füssel, U. (2018). 3D-printed steel reinforcement for digital concrete construction – Manufacture, mechanical properties and bond behaviour. Construction and Building Materials, 179, 125-137. https://doi.org/10.1016/j.conbuildmat.2018.05.202
[115] Mechtcherine, V., Nerella, V. N., Will, F., Näther, M., Otto, J., & Krause, M. (2019). Medium-scale digital concrete construction – CONPrint3D concept for on-site, monolithic 3D-printing. Automation in Construction, 107, 102933. https://doi.org/10.1016/j.autcon.2019.102933.
[116] Morel, J.-C., Bui, Q.-B., & Hamard, E. (2012). Weathering and durability of earthen material and structures. In Modern Earth Buildings: Materials, Engineering, Constructions and Applications (pp. 282-303). Woodhead Publishing. https://doi.org/10.1533/9780857096166.2.282
[117] Morrison, J. (2024). Can 3D printing help address the affordable housing crisis in the United States? *Smithsonian Magazine*. Retrieved from https://www.smithsonianmag.com/innovation/can-3d-printing-help-address-affordable-housing-crisis-in-united-states-180983821/
[118] MTS Systems Corporation. (n.d.). Sistemas de prueba electromecánico Exceed®. Retrieved from https://www.mts.com/la/products/materials/static-materials-test-systems/exceed-electromechanical
[119] Mueller, R. P., Fikes, J. C., Case, M. P., Khoshnevis, B., Fiske, M. R., Edmunson, J. E., Kelso, R., Romo, R., & Andersen, C. (2017). Additive construction with mobile emplacement (ACME). 68th International Astronautical Congress (IAC), Adelaide, Australia, 25-29 September 2017. https://www.researchgate.net/profile/Rodrigo-Romo-2/publication/322567924_Additive_Construction_with_Mobile_Emplacement_ACME/lin

ks/5a5ffe7faca2727352458863/Additive-Construction-with-Mobile-Emplacement-ACME.pdf.
[120] Narita, N., Sagisaka, M., Atsushi, I. (2002). Life cycle inventory analysis of CO2 emissions manufacturing commodity plastics in Japan. The International Journal of Life Cycle Assessment 7 (5), 277–282.
[121] Nematollahi, B., Xia, M., & Sanjayan, J. (2018). Effect of type of fiber on inter-layer bond and flexural strengths of extrusion-based 3D printed geopolymer. Materials Science Forum, 939, 155-162. https://doi.org/10.4028/www.scientific.net/MSF.939.155.
[122] Nguyen, V. T., Lee, S. Y., Yoon, S., & Kim, D. J. (2024). A comprehensive study on predicting the elastic modulus and Poisson ratio of hardened cement pastes via micro-scale cement hydration simulations. Case Studies in Construction Materials, 20, e03285. https://doi.org/10.1016/j.cscm.2024.e03285
[123] NZS D4298: 1998. Materials and workmanship for earth buildings. Retrieved from https://cobcode.s3.amazonaws.com/supporting-docs/NZS4298-1998-Materials_and_Workmanship_For_Earth_Buildings.pdf
[124] Pacheco-Torgal, F., & Jalali, S. (2011). Earth construction: Lessons from the past for future eco-efficient construction. Construction and Building Materials, 29(1), 512-519. https://doi.org/10.1016/j.conbuildmat.2011.10.054.
[125] Panda, B., Lim, J. H., & Tan, M. J. (2019). Mechanical properties and deformation behaviour of early age concrete in the context of digital construction. Composites Part B: Engineering, 165, 563-571. https://doi.org/10.1016/j.compositesb.2019.02.040
[126] Panda, B., Paul, S. C., Hui, L. J., Tay, Y. W. D., & Tan, M. J. (2017). Additive manufacturing of geopolymer for sustainable built environment. Journal of Cleaner Production, 167, 281-288. https://doi.org/10.1016/j.jclepro.2017.08.165.
[127] Panda, B., Paul, S. C., & Tan, M. J. (2017). Anisotropic mechanical performance of 3D printed fiber reinforced sustainable construction material. Materials Letters, 209, 146-149. https://doi.org/10.1016/j.matlet.2017.07.123.
[128] Panda, B., Ruan, S., Unluer, C., & Tan, M. J. (2019). Improving the 3D printability of high volume fly ash mixtures via the use of nano attapulgite clay. Composites Part B: Engineering, 165, 75-83. https://doi.org/10.1016/j.compositesb.2018.11.109.
[129] Panda, B., & Tan, M. J. (2018). Experimental study on mix proportion and fresh properties of fly ash based geopolymer for 3D concrete printing. Ceramics International, 44(9), 10258-10265. https://doi.org/10.1016/j.ceramint.2018.03.031.
[130] Panda, B., Unluer, C., & Tan, M. J. (2018). Investigation of the rheology and strength of geopolymer mixtures for extrusion-based 3D printing. Cement and Concrete Composites, 94, 307-314. https://doi.org/10.1016/j.cemconcomp.2018.10.002.
[131] Paritala, S., Singaram, K. K., Bathina, I., Khan, M. A., & Jyosyula, S. K. R. (2023). Rheology and pumpability of mix suitable for extrusion-based concrete 3D printing – A review. Construction and Building Materials, 402, 132962. https://doi.org/10.1016/j.conbuildmat.2023.132962
[132] Patty, & Anne, L. (2004). PLA or polylactic acid. O Ecotextiles. Retrieved from https://oecotextiles.blog/category/fibers/pla-or-polylactic-acid/
[133] Peels, J. (2021). Holcim and COBOD build first 3D printed house in Kenya. 3DPrint.com. Retrieved from https://3dprint.com/287480/holcim-and-cobod-build-first-3d-printed-house-in-kenya/
[134] Perrot, A., Jacquet, Y., Caron, J. F., Mesnil, R., Ducoulombier, N., De Bono, V., Sanjayan, J., Ramakrishnan, S., Kloft, H., Gosslar, J., Muthukrishnan, S., Mechtcherine, V., Wangler, T., Provis, J. L., Dörfler, K., Krakovska, E., Roussel, N., & Keita, E. (2024). Snapshot on 3D printing with alternative binders and materials: Earth, geopolymers, gypsum and low carbon concrete. Cement and Concrete Research, 185, 107651.

https://doi.org/10.1016/j.cemconres.2024.107651.
[135] Perrot, A., Rangeard, D., & Courteille, E. (2018). 3D printing of earth-based materials: Processing aspects. Construction and Building Materials, 172, 670-676. https://doi.org/10.1016/j.conbuildmat.2018.04.017
[136] Rangasamy, G., Mani, S., Kolandavelu, S. K. S., Alsoufi, M. S., Ibrahim, A. M. M., Muthusamy, S., Panchal, H., Sadasivuni, K. K., & Elsheikh, A. H. (2021). An extensive analysis of mechanical, thermal and physical properties of jute fiber composites with different fiber orientations. Case Studies in Thermal Engineering, 28, 101612. https://doi.org/10.1016/j.csite.2021.101612
[137] Reckford, J. T. M., & Aki-Sawyerr, Y. (2023). Informal settlements are growing everywhere — here's what we do. World Economic Forum. Retrieved from https://www.weforum.org/stories/2023/08/informal-settlements-are-growing-heres-how-we-provide-everyone-a/
[138] REN21. (2022). Renewables 2022 Global Status Report. Retrieved from https://www.ren21.net/gsr-2022/
[139] Ren, G., Yao, B., Ren, M., Gao, X. (2022). Utilization of natural sisal fibers to manufacture eco-friendly ultra-high performance concrete with low autogenous shrinkage. Journal of Cleaner Production, 332 (2022) 130105, https://doi.org/10.1016/j.jclepro.2021.130105.
[140] Rincher, J. (2023). Around the world in 3D printed buildings. 3DPrint.com. Retrieved from https://3dprint.com/304694/around-the-world-in-3d-printed-buildings/
[141] Rojat, F., Hamard, E., Fabbri, A., Carnus, B., & McGregor, F. (2020). Towards an easy decision tool to assess soil suitability for earth building. Construction and Building Materials, 257, 119544. https://doi.org/10.1016/j.conbuildmat.2020.119544
[142] Ross, L. (2024). 3D printing in construction: Materials, applications, and advantages. Thomasnet. Retrieved from https://www.thomasnet.com/insights/3d-printing-in-construction/?msockid=157ec8478ba8612439fcdc088aba605b
[143] Roussel, N. (2018). Rheological requirements for printable concretes. Cement and Concrete Research, 112, 76-85. https://doi.org/10.1016/j.cemconres.2018.04.005.
[144] Rui, A., Wang, L., Lin, W., & Ma, G. (2023). Experimental study on damage anisotropy of 3D-printed concrete exposed to sulfate attack. Construction and Building Materials, 407, 133590. https://doi.org/10.1016/j.conbuildmat.2023.133590.
[145] Schweiker, M., Endres, E., Gosslar, J., Hack, N., Hildebrand, L., Creutz, M., Klinge, A., Kloft, H., Knaack, U., Mehnert, J., & Roswag-Klinge, E. (2021). Ten questions concerning the potential of digital production and new technologies for contemporary earthen constructions. Building and Environment, 206, 108240. https://doi.org/10.1016/j.buildenv.2021.108240
[146] Scott, C. (2016). Chinese construction company 3D prints an entire two-story house on-site in 45 days. 3DPrint.com. Retrieved from https://3dprint.com/138664/huashang-tengda-3d-print-house/.
[147] Sepasgozar, S. M. E., Shi, A., Yang, L., Shirowzhan, S., & Edwards, D. J. (2020). Additive manufacturing applications for Industry 4.0: A systematic critical review. Buildings, 10(12), 231. https://doi.org/10.3390/buildings10120231.
[148] Servicio Nacional de Meteorología e Hidrología del Perú. (2024). Pronóstico del tiempo para Lima Oeste. Retrieved from https://www.senamhi.gob.pe/main.php?p=pronostico-detalle&dp=lima&localidad=0001
[149] Shahinur, S., & Hasan, M. (2019). Natural Fiber and Synthetic Fiber Composites: Comparison of Properties, Performance, Cost and Environmental Benefits. In Elsevier Inc.. https://doi.org/10.1016/B978-0-12-803581-8.10994-4.
[150] Shakor, P., Sanjayan, J., Nazari, A., & Nejadi, S. (2017). Modified 3D printed powder

to cement-based material and mechanical properties of cement scaffold used in 3D printing. Construction and Building Materials, 138, 398-409. https://doi.org/10.1016/j.conbuildmat.2017.02.037
[151] Shukla, S., & Mittal, A. (2022). Effect of jute fibre reinforcement on strength, thickness and cost of low-volume rural roads. Materials Today: Proceedings, 62(12), 6749-6754. https://doi.org/10.1016/j.matpr.2022.04.848
[152] Siddika, A., Al Mamun, M. A., Ferdous, W., Saha, A. K., & Alyousef, R. (2019). 3D-printed concrete: Applications, performance, and challenges. Journal of Sustainable Cement-Based Materials, 9(3), 127-164. https://doi.org/10.1080/21650373.2019.1705199.
[153] Siddique, R., & Mehta, A. (2014). Effect of carbon nanotubes on properties of cement mortars. Construction and Building Materials, 50, 116-129. http://dx.doi.org/10.1016/j.conbuildmat.2013.09.019.
[154] Sikora, P., Chougan, M., & Stephan, D. (2021). The effects of nano- and micro-sized additives on 3D printable cementitious and alkali-activated composites: A review. Applied Nanoscience, 12(2022), 805-823. https://doi.org/10.1007/s13204-021-01738-2
[155] Sikora, P., Chung, S.-Y., Liard, M., Lootens, D., Dorn, T., Kamm, P. H., Stephan, D., & Abd Elrahman, M. (2021). The effects of nanosilica on the fresh and hardened properties of 3D printable mortars. Construction and Building Materials, 281, 122574. https://doi.org/10.1016/j.conbuildmat.2021.122574.
[156] Singh, A. K., Kumar, M., & Mitra, S. (2018). Carbon footprint and energy use in jute and allied fibre production. The Indian Journal of Agricultural Sciences, 88(8), 1305-1311. https://doi.org/10.56093/ijas.v88i8.82579.
[157] Silva, G., Ñañez, R., Zavaleta, D., Burgos, V., Kim, S., Ruiz, G., Pando, M. A., Aguilar, R., & Nakamatsu, J. (2022). Eco-friendly additive construction: Analysis of the printability of earthen-based matrices stabilized with potato starch gel and sisal fibers. Construction and Building Materials, 347, 128556. https://doi.org/10.1016/j.conbuildmat.2022.128556
[158] Sonebi, M., Abdalqader, A., Amziane, S., Dvorkin, L., Ghorbel, E., Kenai, S., Khatib, J., Lushnikova, N., & Perrot, A. (2022). Trends and opportunities of using local sustainable building materials in the Middle East and North Africa region. RILEM Technical Letters, 7, 127-138. https://doi.org/10.21809/rilemtechlett.2022.169.
[159] Song, H., Liu, J., He, K., & Ahmad, W. (2021). A comprehensive overview of jute fiber reinforced cementitious composites. Case Studies in Construction Materials, 15, e00724. https://doi.org/10.1016/j.cscm.2021.e00724
[160] Soroushian, P. (2000). Reinforcing effects of processed cellulose fibers in mortar (stucco), thin sheet products, and concrete. Symposium Paper, 190, 203-212. https://doi.org/10.14359/5729.
[161] Soroushian, P., & Ravanbakhsh, S. (1998). Control of plastic shrinkage cracking with specialty cellulose fibers. Materials Journal, 95(4), 429-435. https://doi.org/10.14359/385.
[162] Sosa, M., Centeno, Y., & Águila, I. (n.d.). Desempeño del concreto reforzado con fibras de sisal para la producción de componentes constructivos. Performance of the Reinforced Concrete with Sisal Fiber for the Production of Building Components.
[163] Souza, M. T., Ferreira, I. M., de Moraes, E. G., Senff, L., & de Oliveira, A. P. N. (2020). 3D printed concrete for medium-scale buildings: An overview of rheology, printing parameters, chemical admixtures, reinforcements, and economic and environmental prospects. Journal of Building Engineering, 32, 101833. https://doi.org/10.1016/j.jobe.2020.101833.
[164] SQ4D LLC. (2024). Largest 3D printed house as of August, 2022. Retrieved from https://www.sq4d.com/islandia-print/
[165] Sun, X., Zhou, J., Wang, Q., Shi, J., & Wang, H. (2022). PVA fibre reinforced high-

strength cementitious composite for 3D printing: Mechanical properties and durability. Additive Manufacturing, 49, 102500. https://doi.org/10.1016/j.addma.2021.102500.
[166] Tay, Y. W. D., Ting, G. H. A., Qian, Y., Panda, B., He, L., & Tan, M. J. (2019). Time gap effect on bond strength of 3D-printed concrete. Virtual and Physical Prototyping, 14(1), 104-113. https://doi.org/10.1080/17452759.2018.1500420.
[167] Tay, Y. W. D., Qian, Y., & Tan, M. J. (2019). Printability region for 3D concrete printing using slump and slump flow test. Composites Part B: Engineering, 174, 106968. https://doi.org/10.1016/j.compositesb.2019.106968
[168] Toledo Filho, R.D., de Andrade Silva, F., Fairbairn, E.M.R., de Almeida Melo Filho J. (2009). Durability of compression molded sisal fiber reinforced mortar laminates, Constr. Build. Mater., 23 (6) 2409–2420. https://doi.org/10.1016/j.conbuildmat.2008.10.012
[169] Torgal, F. P., & Jalali, S. (2011). Natural fiber reinforced concrete. In Fibrous and Composite Materials for Civil Engineering Applications (pp. 154-167). Woodhead Publishing. https://doi.org/10.1533/9780857095583.2.154.
[170] Total Kustom. (n.d.). 3D concrete printers. Retrieved December 17, 2024, from http://www.totalkustom.com/3d-concrete-printers.html
[171] Tudela Laura, M. H. (2024). Desarrollo de un concreto para impresión 3D con agregado reciclado proveniente de conchas de abanico (RCA), residuos de construcción y demolición (RCD) y residuos de polietileno tereftalato (RPET). Pontificia Universidad Católica del Perú. https://tesis.pucp.edu.pe/repositorio//handle/20.500.12404/29268.
[172] Tu, H., Wei, Z., Bahrami, A., Kahla, N. B., Ahmad, A., & Özkılıç, Y. (2023). Recent advancements and future trends in 3D concrete printing using waste materials. Developments in the Built Environment, 16, 100187. https://doi.org/10.1016/j.dibe.2023.100187
[173] UTEST Material Testing Equipment. (n.d.). Vicat Test Sets - Setting Time & Consistency. Retrieved from https://www.utest.com.tr/en/23363/Vicat-Test-Sets
[174] Van Damme, H., Zabat, M., Laurent, J.-P., Dudoignon, P., Pantet, A., Gélard, D., & Houben, H. (2010). Nature and distribution of cohesion forces in earthen building materials. In N. Agnew (Ed.), Conservation of ancient sites on the Silk Road: Proceedings of the Second International Conference on the Conservation of Grotto Sites (pp. 181-188). Getty Publications.
[175] Varela, H., Barluenga, G., Perrot, A. (2023a). Extrusion and structural build-up of 3D printing cement pastes with fly ash, nanoclays and VMAs, Cement and Concrete Composites, 142. https://doi.org/10.1016/j.cemconcomp.2023.105217
[176] Varela, H., Barluenga, G., Sonebi, M. (2023b). Rheology characterization of 3D printing mortars with nanoclays and basalt fibers, Materials Today: Proceedings. https://doi.org/10.1016/j.matpr.2023.07.151.
[177] Varela, H., Pimentel Tinoco, M., Mendoza Reales, O. A., Dias Toledo Filho, R., & Barluenga, G. (2024). Sisal fiber reinforced mortar for 3D printing applications in construction. Procedia Structural Integrity, 64, 1427-1434. https://doi.org/10.1016/j.prostr.2024.09.386.
[178] Veliz Reyes, A., Gomaa, M., Chatzivasileiadi, A., Jabi, W., & Wardhana, N. M. (2018). Computing Craft: Early stage development of a robotically-supported 3D printing system for cob structures. In A. Kepczynska-Walczak & S. Bialkowski (Eds.), Computing for a better tomorrow (pp. 791-800). Education and research in Computer Aided Architectural Design in Europe. https://doi.org/10.1016/j.addma.2019.04.002.
[179] Walker, P., Keable, R., Martin, J., & Maniatidis, V. (2005). Rammed earth: Design and construction guidelines. IHS BRE. Retrieved from https://researchportal.bath.ac.uk/en/publications/rammed-earth-design-and-construction-guidelines

[180] Walsh, N. P. (2019). World's largest 3D-printed concrete pedestrian bridge completed in China. ArchDaily. Retrieved from https://www.archdaily.com/909534/worlds-largest-3d-printed-concrete-pedestrian-bridge-completed-in-china
[181] Wang, X., Jia, L., Jia, Z., Zhang, C., Chen, Y., Ma, L., Wang, Z., Deng, Z., & Banthia, N. (2022). Optimization of 3D printing concrete with coarse aggregate via proper mix design and printing process. Journal of Building Engineering, 56, 104745. https://doi.org/10.1016/j.jobe.2022.104745
[182] WASP. (n.d.). https://www.3dwasp.com/en/about-us/
[183] Weismann, A., & Bryce, K. (2006). Building with cob: A step-by-step guide. Green Books. Retrieved from https://archive.org/details/buildingwithcobs0000weis
[184] Weng, Y., Li, M., Tan, M. J., & Qian, S. (2018). Design 3D printing cementitious materials via Fuller Thompson theory and Marson-Percy model. Construction and Building Materials, 163, 600-610. https://doi.org/10.1016/j.conbuildmat.2017.12.112.
[185] Williams, A. (2023). Earthquake-resistant house 3D printed in just 26 hours. New Atlas. Retrieved from https://newatlas.com/architecture/progreso-3d-printed-house/
[186] Wohlers Associates. (2022). Wohlers Specialty Report on Construction. Retrieved from https://wohlersassociates.com/product/construction2022/
[187] Wolfs, R.J.M., Bos, F.P., Salet, T.A.M. (2019). Hardened properties of 3D printed concrete: The influence of process parameters on interlayer adhesion, Cement and Concrete Research, 119, 132. https://doi.org/10.1016/j.cemconres.2019.02.01
[188] Xia, M., & Sanjayan, J. (2016). Method of formulating geopolymer for 3D printing for construction applications. Materials & Design, 110, 382-390. https://doi.org/10.1016/j.matdes.2016.07.136.
[189] Xiao, J., Ji, G., Zhang, Y., Ma, G., Mechtcherine, V., Pan, J., Wang, L., Ding, T., Duan, Z., & Du, S. (2021). Medium-scale 3D printing concrete technology: Current status and future opportunities. Cement and Concrete Composites, 122, 104115. https://doi.org/10.1016/j.cemconcomp.2021.104115
[190] Yemesegen, E. B., & Memari, A. M. (2023). A review of experimental studies on Cob, Hempcrete, and bamboo components and the call for transition towards sustainable home building with 3D printing. Construction and Building Materials, 399, 132603. https://doi.org/10.1016/j.conbuildmat.2023.132603
[191] Yu, S., Xia, M., Sanjayan, J., Yang, L., Xiao, J., & Du, H. (2021). Microstructural characterization of 3D printed concrete. Journal of Building Engineering, 44, 102948. https://doi.org/10.1016/j.jobe.2021.102948.
[192] Zhang, H., & Xiao, J. (2021). Plastic shrinkage and cracking of 3D printed mortar with recycled sand. Construction and Building Materials, 302, 124405. https://doi.org/10.1016/j.conbuildmat.2021.124405
[193] Zhang, H., Xiao, J., Duan, Z., Zou, S., & Xia, B. (2022). Effects of printing paths and recycled fines on drying shrinkage of 3D printed mortar. Construction and Building Materials, 342, 128007. https://doi.org/10.1016/j.conbuildmat.2022.128007
[194] Zhang, Y., Zhang, Y., & Du, H. (2021). Hardened properties and durability of medium-scale 3D printed cement-based materials. Materials and Structures, 54(1), 45. https://doi.org/10.1617/s11527-021-01632-x.
[195] Zhang, Y., Zhang, Y., She, W., Yang, L., Liu, G., & Yang, Y. (2019). Rheological and harden properties of the high-thixotropy 3D printing concrete. Construction and Building Materials, 201, 278-285. https://doi.org/10.1016/j.conbuildmat.2018.12.061